New results for the two neutrino double beta decay in deformed nuclei with angular momentum projected basis

A. A. Raduta^{a),b)}, A. Escuderos^{c)}, Amand Faessler^{d)}, E. Moya de Guerra^{c)} and P.Sarriguren^{c)}

^{a)} Institute of Physics and Nuclear Engineering, Bucharest, POBox MG6, Romania

^{b)} Department of Theoretical Physics and Mathematics,

Bucharest University, POBox MG11, Romania

^{c)} Instituto de Estructura de la Materia,

Consejo Superior de Investigationes Científicas,

Serrano 123, E-28006 Madrid, Spain and

d) Institut fuer Theoretische Physik, Universitaet Tuebingen, D-72076 Tuebingen, Germany

Abstract

Four nuclei which are proved to be $2\nu\beta\beta$ emitters (76 Ge, 82 Se, 150 Nd, 238 U), and four suspected, due to the corresponding Q-values, to have this property (148 Nd, 154 Sm, 160 Gd, 232 Th), were treated within a proton-neutron quasiparticle random phase approximation (pnQRPA) with a projected spherical single particle basis. The advantage of the present procedure over the ones using a deformed Woods Saxon or Nilsson single particle basis is that the actual pnQRPA states have a definite angular momentum while all the others provide states having only K as a good quantum number. The model Hamiltonian involves a mean field term yielding the projected single particle states, a pairing interaction for alike nucleons and a dipole-dipole proton-neutron interaction in both the particle-hole (ph) and particle-particle (pp) channels. The effect of nuclear deformation on the single beta strength distribution as well as on the double beta Gamow-Teller transition amplitude (M_{GT}) is analyzed. The results are compared with the existent data and with the results from a different approach, in terms of the process half life $T_{1/2}$. The case of different deformations for mother and daughter nuclei is also presented.

PACS numbers: 23.40.Hc, 21.60.Jz, 27.50.+e

I. INTRODUCTION

One of the most exciting nuclear physics subject is that of double beta decay. The interest is generated by the fact that in order to describe quantitatively the decay rate one has to treat consistently the neutrino properties as well as the nuclear structure features. The process may take place in two distinct ways: a) by a $2\nu\beta\beta$ decay the initial nuclear system, the mother nucleus, is transformed in the final stable nuclear system, usually called the daughter nucleus, two electrons and two anti-neutrinos b) by the $0\nu\beta\beta$ process the final state does not involve any neutrino. The latter decay mode is especially interesting since one hopes that its discovery might provide a definite answer to the question whether the neutrino is a Majorana or a Dirac particle. The $0\nu\beta\beta$ decay is an extremely rare process and moreover it is hard to distinguish the electrons emerging from the two processes. For some processes there exists information about the low limits of the process half-lives. Combining this information with the nuclear matrix elements, some conclusions about the upper limits of both neutrino effective mass and effective right-handedness of the electroweak interaction was possible. Unfortunately there are no reliable tests for the nuclear matrix elements involved and therefore some indirect methods should be adopted. It is worth mentioning that the matrix elements which are responsible for neutrinoless double beta decay are similar to those needed for calculating the $2\nu\beta\beta$ decay rate, for which there exists experimental data. Due to this feature an indirect test for the matrix elements used for $0\nu\beta\beta$ is to use those m.e. which describe quantitatively the $2\nu\beta\beta$ decay.

For such reasons many theoreticians focused their efforts in describing consistently the data for $2\nu\beta\beta$ decay. The contributions over several decades have been reviewed by many authors. Instead of enumerating the main steps achieved toward improving the theoretical description we advise the reader to consult few of the review works [1, 2, 3, 4, 5, 6, 7, 8].

It is interesting to note that although none of the double beta emitters is a spherical nucleus most formalisms use a single particle spherical basis. More than 10 years ago, two of us [9] proposed a formalism to describe the process of two neutrinos double beta decay in a projected spherical basis. It was for the first time that a pnQRPA approach for a two body interaction in the ph and pp channels with a deformed single particle basis was performed. Moreover, effects which are beyond the proton-neutron quasiparticle random phase approximations (pnQRPA) have been accounted for by means of a boson expansion proce-

dure. A few years later the influence of nuclear deformation upon the contribution of the spin-flip configurations to the Gamow-Teller double beta transition amplitude, was studied [10]. In the meantime several papers have been devoted to the extension of the pnQRPA procedure to deformed nuclei, the applications being performed for studying the single beta decay properties as well as the double beta decay rates. Thus, pnQRPA approaches using as deformed single particle basis, Nilsson or deformed Woods Saxon states have been formulated[11, 12, 13]. Also a selfconsistent deformed method was formulated where the single particle basis was obtained as eigenstates of a deformed mean field obtained through a Hartree-Fock treatment of a density dependent two body interaction of Skyrme type [12].

The present investigation is, in fact, a continuation of the work from Ref. [9]. Therein the single particle energies were depending linearly on a parameter which simulates the nuclear deformation. By contrast, here the core volume conservation constraint, ignored in the previous paper, determines a nonlinear deformation dependence for single particle energies. Of course, having different single particle energies one expects that the pairing properties and the double beta matrix elements are modified. Another issue addressed in the present paper is whether considering different deformations for the mother and daughter nuclei, modifies significantly the double beta transition amplitude (M_{GT}) . To be more specific, we recall that the standard pnQRPA approach including only the two body interaction in the particle-hole (ph) channel yields a M_{GT} value much larger than the experimental value extracted from the corresponding half-life. Apparently, the desired M_{GT} suppression might be obtained by a suitable choice of the two body interaction in the particle-particle (pp) channel. However, the fitted strength is close to the value where M_{GT} cancels and moreover close to the critical value where the pnQRPA breaks down. It is obvious that increasing the deformation for the daughter nucleus the pnQRPA phonon state is less correlated and therefore the pnQRPA breaking point is pushed toward larger values. In this respect, one may say that the value of the pp interaction strength which reproduces the experimental value for M_{GT} becomes reliable, i.e. the corresponding pnQRPA ground state of the daughter nucleus is stable against adding anharmonic effects.

The formalism and results of the present paper will be presented according to the following plan. In Section II a brief review of the projected spherical single particle basis will be presented. Section III deals with the pnQRPA treatment of a many body Hamiltonian which describes the nuclear states of the mother, daughter and intermediate odd-odd nuclei, involved in the $2\nu\beta\beta$ process. In Section IV, we discuss the results for eight double beta emitters: ⁷⁶Ge, ⁸²Se, ¹⁴⁸Nd ¹⁵⁰Nd, ¹⁵⁴Sm, ¹⁶⁰Gd, ²³²Th, ²³⁸U for which the strength distribution for single β^- and β^+ emission for mother and daughter nuclei,respectively, the M_{GT} and half lives values for the double beta decay process are presented. A short summary and concluding remarks are given in Section V.

II. PROJECTED SINGLE PARTICLE BASIS

In Ref. [14], one of us, (A.A.R.), introduced an angular momentum projected single particle basis which seems to be appropriate for the description of the single particle motion in a deformed mean field generated by the particle-core interaction. This single particle basis has been used to study the collective M1 states in deformed nuclei [15] as well as the rate of double beta process [9, 10]. Recently a new version has been proposed where the deformation dependence of single particle energies is nonlinear and therefore more realistic [16, 17]. In order to fix the necessary notations and to be self-contained, in the present work we describe briefly the main ideas underlying the construction of the projected single particle basis. Also some new properties for the projected basis are pointed out.

The single particle mean field is determined by a particle-core Hamiltonian:

$$\tilde{H} = H_{sm} + H_{core} - M\omega_0^2 r^2 \sum_{\lambda=0,2} \sum_{-\lambda \le \mu \le \lambda} \alpha_{\lambda\mu}^* Y_{\lambda\mu}. \tag{2.1}$$

where H_{sm} denotes the spherical shell model Hamiltonian while H_{core} is a harmonic quadrupole boson (b_{μ}^{+}) Hamiltonian associated to a phenomenological core. The interaction of the two subsystems is accounted for by the third term of the above equation, written in terms of the shape coordinates α_{00} , $\alpha_{2\mu}$. The quadrupole shape coordinates are related to the quadrupole boson operators by the canonical transformation:

$$\alpha_{2\mu} = \frac{1}{k\sqrt{2}} (b_{2\mu}^{\dagger} + (-)^{\mu} b_{2,-\mu}), \tag{2.2}$$

where k is an arbitrary C number. The monopole shape coordinate is to be determined from the volume conservation condition. In the quantized form, the result is:

$$\alpha_{00} = -\frac{1}{4k^2\sqrt{\pi}} \left[5 + \sum_{\mu} (2b_{\mu}^{\dagger}b_{\mu} + (b_{\mu}^{\dagger}b_{-\mu}^{\dagger} + b_{-\mu}b_{\mu})(-)^{\mu}) \right]. \tag{2.3}$$

Averaging \tilde{H} on the eigenstates of H_{sm} , hereafter denoted by $|nljm\rangle$, one obtains a deformed boson Hamiltonian whose ground state is, in the harmonic limit, described by a coherent state

$$\Psi_q = \exp[d(b_{20}^+ - b_{20})]|0\rangle_b, \tag{2.4}$$

with $|0\rangle_b$ standing for the vacuum state of the boson operators and d a real parameter which simulates the nuclear deformation. On the other hand, the average of \tilde{H} on Ψ_g is similar to the Nilsson Hamiltonian [18]. Due to these properties, it is expected that the best trial functions to generate, through projection, a spherical basis are:

$$\Psi_{nlj}^{pc} = |nljm\rangle\Psi_q. \tag{2.5}$$

The upper index appearing in the l.h. side of the above equation suggests that the product function is associated to the particle-core system. The projected states are obtained, in the usual manner, by acting on these deformed states with the projection operator

$$P_{MK}^{I} = \frac{2I+1}{8\pi^2} \int D_{MK}^{I*}(\Omega) \hat{R}(\Omega) d\Omega. \tag{2.6}$$

We consider the subset of projected states:

$$\Phi_{nlj}^{IM}(d) = \mathcal{N}_{nlj}^{I} P_{MI}^{I}[|nljI\rangle\Psi_g] \equiv \mathcal{N}_{nlj}^{I} \Psi_{nlj}^{IM}(d). \tag{2.7}$$

which are orthonormalized.

The main properties of these projected spherical states are: a) They are orthogonal with respect to I and M quantum numbers. b) Although the projected states are associated to the particle-core system, they can be used as a single particle basis. Indeed, when a matrix element of a particle like operator is calculated, the integration on the core collective coordinates is performed first, which results in obtaining a final factorized expression: one factor carries the dependence on deformation and one is a spherical shell model matrix element. c) The connection between the nuclear deformation and the parameter d entering the definition of the coherent state (2.4) is readily obtained by requiring that the strength of the particle-core quadrupole-quadrupole interaction be identical to the Nilsson deformed term of the mean field:

$$\frac{d}{k} = \sqrt{\frac{2\pi}{45}} (\Omega_{\perp}^2 - \Omega_z^2). \tag{2.8}$$

Here Ω_{\perp} and Ω_z denote the frequencies of Nilsson's mean field related to the deformation $\delta = \sqrt{45/16\pi}\beta$ by:

$$\Omega_{\perp} = \left(\frac{2+\delta}{2-\delta}\right)^{1/3}, \ \Omega_z = \left(\frac{2+\delta}{2-\delta}\right)^{-2/3}.$$
(2.9)

The constant k was already defined by Eq.2.2. This is at our disposal since the canonical property of the quoted transformation is satisfied for any value of k. The average of the particle-core Hamiltonian $H' = \tilde{H} - H_{core}$ on the projected spherical states defined by Eq.(2.7) has the expression

$$\epsilon_{nlj}^{I} = \langle \Phi_{nlj}^{IM}(d) | H' | \Phi_{nlj}^{IM}(d) \rangle = \epsilon_{nlj} - \hbar \omega_0 (N + \frac{3}{2}) C_{I0I}^{j2j} C_{1/201/2}^{j2j} \frac{(\Omega_{\perp}^2 - \Omega_{z}^2)}{3}
+ \hbar \omega_0 (N + \frac{3}{2}) \left[1 + \frac{5}{2d^2} + \frac{\sum_{J} (C_{I-I0}^{jIJ})^2 I_{J}^{(1)}}{\sum_{J} (C_{I-I0}^{jIJ})^2 I_{J}^{(0)}} \right] \frac{(\Omega_{\perp}^2 - \Omega_{z}^2)^2}{90}.$$
(2.10)

Here we used the Condon-Shortley convention and notation for the Clebsch Gordan coefficients $C_{m_1m_2m}^{j_1j_1j}$. $I_J^{(k)}$ stands for the following integral

$$I_J^{(i)} = \int_0^1 P_J(x) [P_2(x)]^i exp[d^2 P_2(x)] dx, \ i = 0, 1.$$
 (2.11)

where $P_J(x)$ denotes the Legendre polynomial of rank J. It is worth mentioning that the norms for the core's projected states as well as the matrix elements of any boson operator on these projected states can be fully determined once the overlap integrals defined in (2.11), are known [17]. Since the core contribution does not depend on the quantum numbers of the single particle energy level, it produces a shift for all energies and therefore is omitted in Eq.(2.10). However, when the ground state energy variation against deformation is studied, this term must be included.

The first term from (2.10) is, of course, the single particle energy for the spherical shell model state $|nljm\rangle$. The second term, linear in the deformation parameter d, is the only one considered in the previous works devoted to the double beta decay of deformed nuclei within a projected spherical basis formalism. The third term from Eq.(2.10) is determined by the monopole-monopole particle-core coupling term after implementing the volume conservation condition. This term is the one responsible for the nonlinear deformation dependence of ϵ_{nlj}^I . The energies ϵ_{nlj}^I are represented as function of the deformation parameter d, for the major shells with N equal to 3 and 4, in Fig. 1. We remark that the energies shown in the above mentioned plot depend on deformation in a different manner than those obtained in Ref. [14]. Indeed, therein they depend linearly on deformation, while here non-linear effects are

present. The difference between the two sets of energies is caused by the fact that here the volume conservation condition was used for the monopole shape coordinate, while in Ref.[14] this term is ignored. The difference in the single particle energies is expected to cause significant effects on the single and double beta transition probabilities. Actually, this is the main motivation for the present investigation.

As shown in Fig. 1, the dependence of the new single particle energies on deformation is similar to that shown by the Nilsson model[18].

Although the energy levels are similar to those of the Nilsson model, the quantum numbers in the two schemes are different. Indeed, here we generate from each j a multiplet of (2j+1) states distinguished by the quantum number I, which plays the role of the Nilsson quantum number Ω , runs from 1/2 to j and moreover the energies corresponding to the quantum numbers K and -K are equal to each other. On the other hand, for a given I there are 2I+1 degenerate sub-states while the Nilsson states are only double degenerate. As explained in Ref.[14], the redundancy problem can be solved by changing the normalization of the model functions:

$$\langle \Phi_{\alpha}^{IM} | \Phi_{\alpha}^{IM} \rangle = 1 \Longrightarrow \sum_{M} \langle \Phi_{\alpha}^{IM} | \Phi_{\alpha}^{IM} \rangle = 2.$$
 (2.12)

Due to this weighting factor the particle density function is providing the consistency result that the number of particles which can be distributed on the (2I+1) sub-states is at most 2, which agrees with the Nilsson model. Here α stands for the set of shell model quantum numbers nlj. Due to this normalization, the states Φ_{α}^{IM} used to calculate the matrix elements of a given operator should be multiplied with the weighting factor $\sqrt{2/(2I+1)}$. The role of the core component is to induce a quadrupole deformation for the matrix elements of the operators acting on particle degrees of freedom. Indeed, for any such an operator the following factorization holds:

$$\langle \Phi_{nlj}^{I} || T_k || \Phi_{n'l'j'}^{I'} \rangle = f_{nljI}^{n'l'j'I'} \langle nlj || T_k || n'l'j' \rangle. \tag{2.13}$$

The factor f carries the dependence on the deformation parameter d while the other factor is just the reduced matrix elements corresponding to the spherical shell model states. For details we advise the reader to consult Refs.[14, 17].

Concluding, the projected single particle basis is defined by Eq. (2.7). Although these states are associated to a particle-core system, they can be used as a single particle basis due to the properties mentioned above.

Therefore, the projected states might be thought of as eigenstates of an effective rotational invariant fermionic one-body Hamiltonian H_{eff} , with the corresponding energies given by Eq.(2.10).

$$H_{eff}\Phi_{\alpha}^{IM} = \epsilon_{\alpha}^{I}(d)\Phi_{\alpha}^{IM}.$$
 (2.14)

This definition should be supplemented by the request that the matrix elements of any operator between states Φ_{α}^{IM} and $\Phi_{\alpha'}^{I'M'}$, are given by Eq. (2.13). Due to these features, these states can be used as single particle basis to treat many body Hamiltonians which involve one-body operators. This is the case of Hamiltonians with two body separable forces. As a matter of fact, such a type of Hamiltonian is used in the present paper.

According to our remark concerning the use of the projected spherical states for describing the single particle motion, the average values ϵ^I_{nlj} may be viewed as approximate expressions for the single particle energies in deformed Nilsson orbits[18]. We may account for the deviations from the exact eigenvalues by considering, later on, the exact matrix elements of the two body interaction when a specific treatment of the many body system is applied.

Few words about the vibrational limit, $d \to 0$, for the projected basis are necessary. It can be proved that the following relations hold:

$$\lim_{d\to 0} \Psi_{nlj}^{IM} = \delta_{I,j} |nljM\rangle |0\rangle_{b},$$

$$\lim_{d\to 0} \left(\mathcal{N}_{nlj}^{I}\right)^{-1} = \delta_{I,j},$$

$$\lim_{d\to 0} \langle \Phi_{nlj}^{j} || T_{k} || \Phi_{n'l'j'}^{j'}\rangle = \langle nlj || T_{k} || n'l'j'\rangle,$$

$$\lim_{d\to 0} \epsilon_{nlj}^{j} = \epsilon_{nlj}.$$
(2.15)

Note that in the limit $d \to 0$, the norms of the states with $I \neq j$ are not defined while the limit of the I=j state, normalized to unity, is just the product state $|nljM\rangle|0\rangle_b$. Indeed, the fourth equation (2.15) is fulfilled by neglecting a small quantity $(\frac{5}{8\pi k^2})$ caused by the zero point motion term of the monopole-monopole particle-core interaction. Although in the limit $d \to 0$ the norm of the states $I \neq j$ is not defined, the limit of Φ_{nlj}^{IM} , with $I \neq j$, exists. However, the corresponding energies are not identical to but very close to the spherical shell model state energy.

$$\lim_{d\to 0} \epsilon_{nlj}^{I} = \epsilon_{nlj} + \hbar\omega_0(N + \frac{3}{2}) \left(\frac{5}{2} + \frac{1}{2} \left(j - I + \frac{1}{2} (1 - (-)^{j-I})\right)\right) \frac{1}{4\pi k^2}, \ j \neq I.$$
 (2.16)

Indeed, this term should be compared with the spherical oscillator energy $((N+\frac{3}{2})\hbar\omega_0)$ from

 ϵ_{nlj} . Since the factor $\frac{1}{4\pi k^2}$ is very small (see Table 1) the correction of the shell model term is negligible.

Due to the properties mentioned above, we may state that in the vibrational limit, $d \to 0$, the projected spherical basis goes to the spherical shell model basis.

To complete our description of the projected single particle basis, we recall a fundamental result obtained in Ref.[17], concerning the product of two single particle states which comprises a product of two core components. Therein we have proved that the matrix elements of a two body interaction corresponding to the present scheme are very close to the matrix elements corresponding to spherical states projected from a deformed product state with one factor as a product of two spherical single particle states, and a second factor consisting of a common collective core wave function. The small discrepancies of the two types of matrix elements could be washed out by using slightly different strengths for the two body interaction in the two methods.

III. THE MODEL HAMILTONIAN AND ITS PNQRPA APPROACH

As we already stated, in the present work we are interested to describe the Gamow-Teller two neutrino double beta decay of an even-even deformed nucleus. In our treatment the Fermi transitions, contributing about 20% and the "forbidden" transitions are ignored which is a reasonable approximation for the two neutrino double beta decay in medium and heavy nuclei. Customarily, the $2\nu\beta\beta$ process is conceived as two successive single β^- transitions. The first transition connects the ground state of the mother nucleus to a magnetic dipole state 1⁺ of the intermediate odd-odd nucleus which subsequently decays to the ground state of the daughter nucleus. Going beyond the pnQRPA procedure by means of the boson expansion procedure we were able to consider the process leaving the final nucleus in an excited collective state [19]. Such processes are not treated in the present paper. The states, mentioned above, involved in the $2\nu\beta\beta$ process are described by the following many body Hamiltonian:

$$H = \sum \frac{2}{2I+1} (\epsilon_{\tau\alpha I} - \lambda_{\tau\alpha}) c_{\tau\alpha IM}^{\dagger} c_{\tau\alpha IM} - \sum \frac{G_{\tau}}{4} P_{\tau\alpha I}^{\dagger} P_{\tau\alpha I'} + 2\chi \sum \beta_{\mu}^{-}(pn) \beta_{-\mu}^{+}(p'n') (-)^{\mu} - 2\chi_{1} \sum P_{1\mu}^{-}(pn) P_{-\mu}^{+}(p'n') (-)^{\mu}.$$
(3.1)

The operator $c_{\tau\alpha IM}^{\dagger}(c_{\tau\alpha IM})$ creates (annihilates) a particle of type τ (=p,n) in the state Φ_{α}^{IM} , when acting on the vacuum state $|0\rangle$. In order to simplify the notations, hereafter the set of quantum numbers $\alpha(=nlj)$ will be omitted. The two body interaction consists of three terms, the pairing, the dipole-dipole particle hole (ph) and the particle-particle (pp) interactions. The corresponding strengths are denoted by G_{τ}, χ, χ_1 , respectively. All of them are separable interactions, with the factors defined by the following expressions:

$$P_{\tau I}^{\dagger} = \sum_{M} \frac{2}{2I+1} c_{\tau IM}^{\dagger} c_{\tau IM}^{\dagger},$$

$$\beta_{\mu}(pn) = \sum_{M,M'} \frac{\sqrt{2}}{\hat{I}} \langle pIM | \sigma_{\mu} | nI'M' \rangle \frac{\sqrt{2}}{\hat{I}'} c_{pIM}^{\dagger} c_{nI'M'},$$

$$P_{1\mu}^{-}(pn) = \sum_{M,M'} \frac{\sqrt{2}}{\hat{I}} \langle pIM | \sigma_{\mu} | nI'M' \rangle \frac{\sqrt{2}}{\hat{I}'} c_{pIM}^{\dagger} c_{nI'M'}^{\dagger}.$$
(3.2)

The remaining operators from Eq.(3.1) can be obtained from the above defined operators by hermitian conjugation.

The one body term and the pairing interaction terms are treated first through the standard BCS formalism and consequently replaced by the quasiparticle one body term $\sum_{\tau IM} E_{\tau} a_{\tau IM}^{\dagger} a_{\tau IM}$. In terms of quasiparticle creation $(a_{\tau IM}^{\dagger})$ and annihilation $(a_{\tau IM})$ operators, related to the particle operators by means of the Bogoliubov-Valatin transformation, the two body interaction terms, involved in the model Hamiltonian, can be expressed just by replacing the operators (3.2) by their quasiparticle images:

$$\beta_{\mu}^{-}(k) = \sigma_{k} A_{1\mu}^{\dagger}(k) + \bar{\sigma}_{k} A_{1,-\mu}(k)(-)^{1-\mu} + \eta_{k} B_{1\mu}^{\dagger}(k) - \bar{\sigma}_{k} B_{1,-\mu}(k)(-)^{1-\mu},$$

$$\beta_{\mu}^{+}(k) = -\left[\bar{\sigma}_{k} A_{1\mu}^{\dagger}(k) + \sigma_{k} A_{1,-\mu}(k)(-)^{1-\mu} - \bar{\eta}_{k} B_{1\mu}^{\dagger}(k) + \sigma_{k} B_{1,-\mu}(k)(-)^{1-\mu}\right],$$

$$P_{1\mu}^{-}(k) = \eta_{k} A_{1\mu}^{\dagger}(k) - \bar{\eta}_{k} A_{1,-\mu}(k)(-)^{1-\mu} - \sigma_{k} B_{1\mu}^{\dagger}(k) + \bar{\sigma}_{k} B_{1,-\mu}(k)(-)^{1-\mu},$$

$$P_{\mu}^{+}(k) = -\left[-\bar{\eta}_{k} A_{1\mu}^{\dagger}(k) + \eta_{k} A_{1,-\mu}(k)(-)^{1-\mu} + \bar{\sigma}_{k} B_{1\mu}^{\dagger}(k) - \sigma_{k} B_{1,-\mu}(k)(-)^{1-\mu}\right]. \quad (3.3)$$

In the above equations the argument "k" stands for the proton-neutron state (p,n). Here, the usual notations for the dipole two quasiparticle and quasiparticle density operator have been used:

$$A_{1\mu}^{\dagger}(pn) \; = \; \sum_{m_p,m_n} C_{m_p \; m_n \; \mu}^{I_p \; I_n \; 1} a_{pI_p m_p}^{\dagger} a_{nI_n m_n}^{\dagger},$$

$$B_{1\mu}^{\dagger}(pn) = \sum_{m_n, m_n} C_{m_p - m_n \mu}^{I_p I_n 1} a_{pI_p m_p}^{\dagger} a_{nI_n m_n} (-)^{I_n - m_n}.$$
(3.4)

The coefficients σ and η are simple expressions of the reduced matrix elements of the Pauli matrix σ and U and V coefficients:

$$\sigma_{k} = \frac{2}{\hat{1}\hat{I}_{n}} \langle I_{p}||\sigma||I_{n}\rangle U_{I_{p}}V_{I_{n}}, \quad \bar{\sigma}_{k} = \frac{2}{\hat{1}\hat{I}_{n}} \langle I_{p}||\sigma||I_{n}\rangle V_{I_{p}}U_{I_{n}},$$

$$\eta_{k} = \frac{2}{\hat{1}\hat{I}_{n}} \langle I_{p}||\sigma||I_{n}\rangle U_{I_{p}}U_{I_{n}}, \quad \bar{\eta}_{k} = \frac{2}{\hat{1}\hat{I}_{n}} \langle I_{p}||\sigma||I_{n}\rangle V_{I_{p}}V_{I_{n}},$$

$$(3.5)$$

The quasiparticle Hamiltonian is further treated within the proton-neutron random phase approximation (pnQRPA), i.e. one determines the operator

$$\Gamma_{1\mu}^{\dagger} = \sum_{k} [X(k)A_{1\mu}^{\dagger}(k) - Y(k)A_{1,-\mu}(k)(-)^{1-\mu}], \tag{3.6}$$

which satisfies the restrictions:

$$[\Gamma_{1\mu}, \Gamma_{1\mu'}^{\dagger}] = \delta_{\mu,\mu'}, \quad [H_{qp}, \Gamma_{1\mu}^{\dagger}] = \omega \Gamma_{1\mu}^{\dagger}. \tag{3.7}$$

These operator equations yield a set of algebraic equations for the X (usually called forward going) and Y (named back-going) amplitudes:

$$\begin{pmatrix} A & \mathcal{B} \\ -\mathcal{B} & -\mathcal{A} \end{pmatrix} \begin{pmatrix} X \\ Y \end{pmatrix} = \omega \begin{pmatrix} X \\ Y \end{pmatrix}, \tag{3.8}$$

$$\sum_{k} [|X(k)|^2 - |Y(k)|^2] = 1.$$
(3.9)

The pnQRPA matrices \mathcal{A} and \mathcal{B} have analytical expressions:

$$\mathcal{A}_{k,k'} = (E_p + E_n)\delta_{pp'}\delta_{nn'} + 2\chi(\sigma_k\sigma_{k'} + \bar{\sigma}_k\bar{\sigma}_{k'}) - 2\chi_1(\eta_k\eta_{k'} + \bar{\eta}_k\bar{\eta}_{k'}),$$

$$\mathcal{B}_{k,k'} = 2\chi(\bar{\sigma}_k\sigma_{k'} + \sigma_k\bar{\sigma}_{k'}) + 2\chi_1(\bar{\eta}_k\eta_{k'} + \eta_k\bar{\eta}_{k'}).$$
(3.10)

All quantities involved in the pnQRPA matrices have been already defined. Note that the proton and neutron quasiparticle energies are denoted in an abbreviated manner by E_p and E_n , respectively.

As can be seen from Eq. (3.1) the ph interaction is repulsive while the pp interaction has an attractive character. Due to this feature, for a critical value of χ_1 the lowest root of

the pnQRPA equations may become imaginary. Suppose that χ_1 is smaller than its critical value and therefore all RPA solutions (i.e. ω) are real numbers and ordered as:

$$\omega_1 \le \omega_2 \le \dots \le \omega_{N_s}. \tag{3.11}$$

Here N_s stands for the total number of the proton-neutron pair states whose angular momenta can couple to 1^+ and moreover their quantum numbers n, l are the same. Hereafter the phonon amplitudes X and Y will be accompanied by a lower index "i" suggesting that they correspond to the energy ω_i .

Since our single particle basis states depend on the deformation parameter d, so do the pnQRPA energies and amplitudes. The pnQRPA ground state (the vacuum state of the RPA phonon operator) describes an even-even system which might be alternatively the mother or the daughter nucleus. In the two cases the gauge and nuclear deformation properties are different which results in determining distinct pnQRPA phonon operators acting on different vacua describing the mother and daughter ground states, respectively. Therefore, one needs an additional index distinguishing the phonon operators of the mother and daughter nuclei. The single phonon states are defined by the equations:

$$|1_{j,k}\rangle = \Gamma_{i,k}^{\dagger}|0\rangle_{j}, \ j = i, f; \ k = 1, 2, ...N_{s}.$$
 (3.12)

Here the indices i and f stand for initial (mother) and final (daughter) nuclei, respectively. This equation defines two sets of non-orthogonal states describing the neighboring odd-odd nucleus. The states of the first set may be fed by a beta minus decay of the ground state of the mother nucleus while the states of the second set are populated with a beta plus transition operator from the ground state of the daughter nucleus.

If the energy carried by leptons in the intermediate state is approximated by the sum of the rest energy of the emitted electron and half the Q-value of the double beta decay process

$$\Delta E = m_e c^2 + \frac{1}{2} Q_{\beta\beta},\tag{3.13}$$

the reciprocal value of the $2\nu\beta\beta$ half life can be factorized as:

$$(T_{1/2}^{2\nu\beta\beta})^{-1} = F|M_{GT}(0_i^+ \to 0_f^+)|^2, \tag{3.14}$$

where F is an integral on the phase space, independent of the nuclear structure, while M_{GT} stands for the Gamow-Teller transition amplitude and has the expression [43]:

$$M_{GT} = \sqrt{3} \sum_{kk'} \frac{i\langle 0||\beta_i^+||1_k\rangle_{ii}\langle 1_k|1_{k'}\rangle_{ff}\langle 1_{k'}||\beta_f^+||0\rangle_f}{E_k + \Delta E + E_{1+}}.$$
 (3.15)

In the above equation, the denominator consists of three terms: a) ΔE , which was already defined, b) the average value of the k-th pnQRPA energy normalized to the particular value corresponding to k=1, i.e.

$$E_k = \frac{1}{2}(\omega_{i,k} + \omega_{f,k}) - \frac{1}{2}(\omega_{i,1} + \omega_{f,1}), \tag{3.16}$$

and c) the experimental energy for the lowest 1⁺ state. The indices carried by the transition operators indicate that they act in the space spanned by the pnQRPA states associated to the initial (i) or final (f) nucleus. Details about the overlap matrix of the single phonon states in the mother and daughter nuclei are given in Appendix A.

Before closing this section we would like to say a few words about what is specific to our formalism. As we mentioned before the pnQRPA matrices depend on the deformation parameter and therefore the RPA energies and states depend on deformation. Moreover, in the case that the mother and daughter nuclei are characterized by different nuclear deformations the RPA output for the two nuclei are affected differently by deformation. These features make the pnQRPA formalism build up with a deformed single particle basis quite tedious. Besides these difficulties, one should keep in mind the fact that the usual approaches define the states from the intermediate odd-odd nucleus not as a state of angular momentum 1 but states of a definite K, i.e., $K=\pm 1,0.$ Under such circumstances from the pnQRPA states, the components of good angular momentum are to be projected out. This operation is usually performed in an approximative way, (by transposing the result obtained in the intrinsic frame, to the laboratory frame of reference) which might be justified only in the strong coupling regime. Unfortunately, the double beta emitters are only moderately deformed, which makes the approximation validity, questionable. Actually this is the reason why the answer to the question of how much the results obtained with deformed single particle basis differ from the ones obtained with projected many body RPA state, is not yet known.

By contrast, since our single particle states are projected spherical states, the RPA formalism is fully identical to that one which is usually employed for spherical nuclei. Since in the vibrational limit, $(d \to 0)$, our basis goes to the spherical shell model basis, one may say that the present formalism provides a unified description of spherical and deformed nuclei.

IV. NUMERICAL RESULTS

The formalism described in the previous sections was applied to eight nuclei among which four are proved to be double beta emitters (76 Ge, 82 Se, 150 Nd, 238 U) [22] and four suspected, due to the corresponding $Q_{\beta\beta}$ value, to have this property.

The spherical shell model parameters are those given in Ref. [24], i.e.

$$\hbar\omega_0 = 41A^{-1/3}, \quad C = -2\hbar\omega_0\kappa, \quad D = -\hbar\omega_0\mu. \tag{4.1}$$

For the proton system, the pair of strength parameters (κ, μ) takes the values (0.08;0.) for 76 Ge, 76 Se, 82 Se, 82 Kr, (0.0637;0.6) for 148,150 Nd, $^{148-154}$ Sm, 154,160 Gd, 160 Dy, (0.0577;0.65) for 232 Th, 232,238 U, 238 Pu, while for the neutron systems of the three groups of nuclei mentioned above, the values are (0.08;0.), (0.0637,0.42), (0.0635;0.325), respectively.

The projected spherical single particle basis, used in our calculations, depend on another two parameters, the deformation d and the factor k of the transformation (2.2) relating the boson operators with the quadrupole collective coordinate, according to Eq. (2.2). These were fixed as follows. For the lightest nuclei, Ge, Se, Kr, involved in the process of the double beta decay, the two parameters were taken so that the relative energies of the states $|1f\frac{7}{2}\frac{7}{2}\rangle$ and $|1d\frac{5}{2}\frac{1}{2}\rangle$ as well as the lowest root of the pnQRPA equations with a QQ interaction included, reproduces the relative energy of $\Omega = \frac{7}{2}$ and $\Omega = \frac{1}{2}$ Nilsson states, in the N=3 major shell, and the experimental value for the first collective 2^+ state. The d and k parameters for ¹⁵⁴Sm and its double beta partner ¹⁵⁴Gd were taken equal to those used in a previous publication [17], to describe the M1 states of the mother nucleus. As for the remaining nuclei considered in this paper, the corresponding d and k parameters are the same as in Ref.[25, 26] where one of us (A. A. R.) described phenomenologically the spectroscopic properties of the major rotational bands.

The BCS calculations have been performed within a single particle space restricted so that at least the states from the proton and neutron major open shells are included. Although the single particle energies depend on deformations here we keep calling major shell a set of states having the same quantum number n, according to Eq.(2.7). This truncation criterion defines an energy interval for single particle states. Of course, due to the level crossing caused by deformation, also states from the lower proton and upper neutron major shells, lying in the energy interval defined before, are included in the single particle space. Since

only the proton-neutron pair of states characterized by the same orbital angular momenta, participate in single beta decay processes, the single particle spaces for proton and neutron systems are to be the same. It is well understood that the corresponding energies for protons and neutrons are however different from each others for heavy isotopes, due to the mass dependence of the single particle mean field strength parameters (4.1).

Pairing strengths have been fixed so that the mass differences of the neighboring even-even nuclei are reproduced. The results are listed in Table 1. Their values may be interpolated by a linear function of 1/A both for the mother:

$$G_p = \frac{12.186}{A} + 0.06931, \quad G_n = \frac{8.2745}{A} + 0.11266,$$
 (4.2)

and the daughter nuclei:

$$G_p = \frac{13.806}{A} + 0.06765, \quad G_n = \frac{8.1563}{A} + 0.13455.$$
 (4.3)

Slight deviations from these rules are registered for G_p of ⁷⁶Ge and ⁷⁶Se and G_n of ⁷⁶Ge and ²³⁸Pu. It is interesting to note that although the single particle basis is different from the ones currently used in the literature, the results for the interaction strength is quite close to the standard ones. For example for ¹⁵⁰Sm the above equations are equivalent to $G_p = 22.86/A$, $G_n = 25.624/A$.

As for the proton-neutron two body interactions, their strengths were taken as in Ref.[11] although the single particle basis used therein, is different from ours:

$$\chi = \frac{5.2}{A^{0.7}} \text{MeV}, \quad \chi_1 = \frac{0.58}{A^{0.7}} \text{MeV}.$$
(4.4)

The A dependence for the ph interaction strength has been derived by fitting the position of the GT resonance for 40 Ca, 90 Zr and 208 Pb. The strength χ_1 has been fixed so that the beta decay half lives of the nuclei with $Z \leq 40$ are reproduced. Certainly, the A dependence for χ and χ_1 depends on the mass region to which the considered nucleus belongs as well as on the single particle space. As a matter of fact our results for 76 Ge and 82 Se show that larger values for the ph interaction strength improve the agreement with experimental data. Moreover, our comparison suggests that a certain caution should be taken when the mass dependence given by Eq. (4.4) is considered as in these nucleibe χ and χ_1 parameters cannot be fixed by single beta decay half lives as it is usually done. Once the parameters defining the model Hamiltonian are fixed, the pnQRPA equations have been solved for the mother

and daughter nuclei and the output results have been used in connection with Eq.(3.15) to calculate the GT amplitude of the $2\nu\beta\beta$ process. In the next step, the equation (3.14) provides the double beta half life. The phase space factor F does not depend on the structure of the nuclear states and therefore we take it as given in Ref.[1, 27]. The values for F, used in the present paper, correspond to $g_A = 1.254$. Results for M_{GT} and half lives $(T_{1/2})$ are given in Table 2. There, we also give the strength of the ph and pp interactions produced by Eq.(4.4). For comparison we present also the available experimental data [22, 31, 32, 33] as well as the results of Ref. [28] for $T_{1/2}$.

Nucleus	d	k	$G_p [MeV]$	$G_n [MeV]$	$\chi \ [{ m MeV}]$	g_{pp}
$^{76}\mathrm{Ge}$	1.9	7.1	0.300	0.295	0.35	0.112
$^{76}\mathrm{Se}$			0.295	0.285		
$^{82}\mathrm{Se}$	1.6	3.5	0.150	0.160	0.35	0.112
$^{82}{ m Kr}$			0.210	0.215		
¹⁴⁸ Nd	1.555	10.81	0.118	0.200	0.15733	0.11154
$^{148}\mathrm{Sm}$			0.120	0.220		
¹⁵⁰ Nd	1.952	9.89	0.160	0.150	0.15586	0.11154
$^{150}\mathrm{Sm}$			0.190	0.190		
$^{154}\mathrm{Sm}$	2.29	5.58	0.190	0.134	0.15302	0.11154
$^{154}\mathrm{Gd}$			0.145	0.138		·
$^{160}\mathrm{Gd}$	2.714	4.384	0.160	0.155	0.14898	0.11154
$^{160}\mathrm{Dy}$			0.155	0.160		,
²³² Th	2.51	4.427	0.120	0.183	0.11486	0.11154
$^{232}{ m U}$			0.090	0.225		·
²³⁸ U	2.62	4.224	0.130	0.165	0.080	0.11154
²³⁸ Pu			0.165	0.235		

TABLE I: The pairing and Gamow Teller interactions strength are given in units of MeV. The ratio of the two dipole interaction (particle-hole and particle-particle) strengths, denoted by g_{pp} is given. The list of the deformation parameter d and the factor k of the transformation (2.2) are also presented. The manner in which these parameters were fixed is explained in the text.

Before discussing in extenso the results from Table 2, it is instructive to show the results

Nucleus	χ	g_{pp}	$ m M_{GT}$	$T_{1/2} [yr]$				
				present	exp.	Ref.[28]		
$^{76}\mathrm{Ge} \rightarrow ^{76}\mathrm{Se}$	0.35	0.112	0.222	$5.9 \cdot 10^{20}$	$9.2^{+0.7}_{-0.4} \cdot 10^{20}$ a)	$2.61 \cdot 10^{20}$		
	0.35	0.112	0.149 ^{c)}	$1.32\cdot 10^{21}$	$1.1^{+0.6}_{-0.3} \cdot 10^{21}$ b)			
	0.25	0.11154	0.270	$4.05\cdot10^{20}$				
$^{82}\mathrm{Se} \rightarrow ^{82}\mathrm{Kr}$	0.35	0.112	0.096	$0.963 \cdot 10^{20}$	$1.1^{+0.8}_{-0.3} \cdot 10^{20} \text{ d}$	$0.848 \cdot 10^{20}$		
	0.16	0.108	0.135	$0.49 \cdot 10^{20}$	$1.0 \pm 0.4 \cdot 10^{20}$ e)			
					$1.3 \pm 0.05 \cdot 10^{20 \text{ f}})$			
$^{148}\mathrm{Nd} \rightarrow ^{148}\mathrm{Sm}$	0.157	0.112	0.392	$2.327 \cdot 10^{19}$		$1.19 \cdot 10^{21}$		
$^{150}\mathrm{Nd} \rightarrow ^{150}\mathrm{Sm}$	0.156	0.11154	0.350	$2.630 \cdot 10^{17}$	$\geq 1.8 \cdot 10^{19} \text{ g}$	$1.66\cdot 10^{19}$		
	0.156	1.50	0.040	$1.98\cdot10^{19}$				
$^{154}\mathrm{Sm} \rightarrow ^{154}\mathrm{Gd}$	0.153	0.11154	0.327	$8.760 \cdot 10^{20}$		$1.49 \cdot 10^{22}$		
$^{160}\mathrm{Gd} \rightarrow ^{160}\mathrm{Dy}$	0.149	0.11154	0.170	$2.013 \cdot 10^{20}$		$2.81 \cdot 10^{21}$		
$^{232}\mathrm{Th} \rightarrow ^{232}\mathrm{U}$	0.11486	0.11154	0.123	$4.240 \cdot 10^{21}$		$4.03 \cdot 10^{21}$		
$^{238}\mathrm{U} \rightarrow^{238}\mathrm{Pu}$	0.080	0.112	0.166	$2.375 \cdot 10^{21}$	$(2.0 \pm 0.6) \cdot 10^{21 \text{ h}}$	$0.914 \cdot 10^{21}$		
	0.11282	0.11154	0.139	$3.340 \cdot 10^{21}$				
	0.08	0.0	0.171	$2.249 \cdot 10^{21}$				

TABLE II: The Gamow-Teller amplitude for $2\nu\beta\beta$ decay, in units of MeV⁻¹ and the corresponding half life $(T_{1/2})$ are listed for several ground to ground transitions. The experimental half lives for the transitions $^{76}\text{Ge} \rightarrow ^{76}\text{Se}$ (a)Ref.[30],b)Ref. [29]), $^{82}\text{Se} \rightarrow ^{82}\text{Kr}$ (d) Ref. [33], e) Ref.[32], f) Ref.[31]), $^{150}\text{Nd} \rightarrow ^{150}\text{Sm}$ (g)Ref.[36]) and $^{238}\text{U} \rightarrow ^{238}\text{Pu}$ (h) Refs. [21, 22, 23, 37]) are also given. In the last column the results from Ref.[28], are given. The parameters χ and g_{pp} are also given. c)For these two cases the mother and daughter nuclei have different deformations, namely $d_i = 1.6$ and $d_f = 1.9$. The parameters χ and g_{pp} are listed in the second and third columns.

concerning the single beta decay properties of the mother and daughter nuclei. Thus, in Figs. 2-9 the beta minus strength of the mother and the beta plus streights of the daughter nuclei, folded with a gaussian having the width equal to 1 MeV, are plotted as function of energy. For the lightest two nuclei, the experimental data are also presented [34, 35].

For pedagogical reasons, for these two nuclei two different ph interaction strengths are alternatively used. In this way one clearly sees that increasing the strength χ , the transition strength is moved to the higher state. Thus, although the peak positions remain the same, since the BCS data are not changed, the first peak looses height while the second one is augmented. The agreement with experimental data is reasonably good. In both mother nuclei the center of the GT resonance is a little bit shifted, backward for 82 Se and forward for 76 Ge. Due to the fragmentation effect caused by the nuclear deformation, the theoretical result for the GT resonance has a shorter, otherwise broader peak than the experimental one. In order to see that a broad peak in the folded beta strength plot means, indeed, a fragmentation of the strength distributed among several pnQRPA states, we show the unfolded strength for 82 Se and 232 Th isotopes in Figs 10 and 11, respectively. For example, in the case of 82 Se, the folded strength exhibits a first fat peak which has a very short maximum before and a "shoulder" on the descending part (see the middle panels of Figs.3). From Fig.10 one sees that to these details correspond pnQRPA states which carry a strength represented by sticks which dominate the grass spread around.

The total strength of the GT resonance is about the same as the corresponding experimental data. However the fragmentation is causing a broad resonance which results in having a shorter peak. This fact might raise the question whether the deformation considered in the present paper is too large. Indeed, the neutron system of ⁸²Se is almost spherical since N (the neutron number) is close to a magic value. Due to this feature we repeated the calculations with a very small d(=0.2) which is close to the spherical limit. As seen from the right panel the height of GT resonance corresponding to the new deformation is close to the experimental result. Since we kept the same parameter for the single particle mean field parameters, e.g for the parameter k defined in Eq. (2.2), the theoretical curve is shifted by about 1 MeV with respect to the experimental data. Of course, the position of the GT resonance depends also on the pairing strengths. The parameters mentioned above where kept the same as for the initial deformation case (d=1.9), in order to judge, by comparison, the effect coming from the nuclear deformation. In conclusion, going from deformed to spherical single particle basis the GT resonance peak is getting higher and the width narrower. Actually when the calculated strength distribution is compared with the experimental data one has to restrict the discussion only to the position of the GT centroid and the total strength, since there is no experimental information about the resonance width. The narrow whith seen, however, in Figs. 2 and 3 is caused by folding a single number indicating the total β^- strength for the GT resonance which has the centroid at a given energy, with a Gaussian having the width equal to 1 MeV.

From the folded beta minus strengths graphs, we see that for heavier double beta emitters there exists a small peak lying above the GT resonance.

Nucleus	1st peak		2nd peak		3rd peak		
	Transition	Strength	Transition	Strength	Transition	Strength	
$^{76}\mathrm{Ge}$	$\nu(4d\frac{5}{2}\frac{3}{2}) \to \pi(4d\frac{5}{2}\frac{1}{2})$	1.084	$\nu(4d\frac{3}{2}\frac{1}{2}) \to \pi(4d\frac{5}{2}\frac{3}{2})$	1.740	$\nu(3f\frac{7}{2}\frac{5}{2}) \to \pi(3f\frac{5}{2}\frac{5}{2})$	1.718	
			$\nu(3f\frac{7}{2}\frac{1}{2}) \to \pi(3f\frac{5}{2}\frac{3}{2})$	3.371			
$^{82}\mathrm{Se}$	$\nu(3f\frac{5}{2}\frac{5}{2}) \to \pi(3f\frac{7}{2}\frac{3}{2})$	1.554	$\nu(3p\frac{3}{2}\frac{3}{2}) \to \pi(3p\frac{3}{2}\frac{1}{2})$	4.501	$\nu(3p\frac{3}{2}\frac{1}{2} \to \pi(3p\frac{3}{2}\frac{3}{2})$	1.686	
					$\nu(3f\frac{7}{2}\frac{3}{2}) \to \pi(3f\frac{5}{2}\frac{3}{2})$	3.310	
$^{148}\mathrm{Nd}$	$\nu(4g\frac{7}{2}\frac{7}{2}) \to \pi(4g\frac{9}{2}\frac{5}{2})$	1.077	$\nu(4g\frac{7}{2}\frac{3}{2}) \to \pi(4g\frac{9}{2}\frac{5}{2})$	1.453			
	$\nu(4g\frac{7}{2}\frac{5}{2}) \to \pi(4g\frac{9}{2}\frac{7}{2})$	1.141	$\nu(4g\frac{9}{2}\frac{5}{2}) \to \pi(4g\frac{7}{2}\frac{3}{2})$	12.437			
			$\nu(4g\frac{9}{2}\frac{5}{2}) \to \pi(4g\frac{7}{2}\frac{7}{2})$	1.015			
$^{150}\mathrm{Nd}$	$\nu(4g\frac{7}{2}\frac{7}{2}) \to \pi(4g\frac{9}{2}\frac{5}{2})$	1.901	$\nu(5h\frac{11}{2}\frac{3}{2}) \to \pi(5h\frac{9}{2}\frac{3}{2})$	1.246	$\nu(4d\frac{5}{2}\frac{1}{2}) \to \pi(4d\frac{3}{2}\frac{3}{2})$	5.386	
			$\nu(4g\frac{7}{2}\frac{5}{2}) \to \pi(4g\frac{9}{2}\frac{3}{2})$	1.178	$\nu(4g\frac{9}{2}\frac{3}{2}) \to \pi(4g\frac{7}{2}\frac{3}{2})$	2.370	
			$\nu(4g\frac{9}{2}\frac{5}{2}) \to \pi(4g\frac{7}{2}\frac{3}{2})$	1.087			
			$\nu(4g\frac{9}{2}\frac{3}{2}) \to \pi(4g\frac{9}{2}\frac{5}{2})$	7.647			
$^{154}\mathrm{Sm}$	$\nu(5f\frac{7}{2}\frac{3}{2}) \to \pi(5f\frac{7}{2}\frac{5}{2})$	1.220	$\nu(4g\frac{7}{2}\frac{1}{2}) \to \pi(4g\frac{7}{2}\frac{3}{2})$	4.214	$\nu(4g\frac{9}{2}\frac{5}{2}) \to \pi(4g\frac{7}{2}\frac{5}{2})$	1.537	
	$\nu(6i\frac{13}{2}\frac{7}{2}) \to \pi(6i\frac{13}{2}\frac{9}{2})$	1.031	$\nu(4d\frac{3}{2}\frac{1}{2}) \to \pi(4d\frac{3}{2}\frac{3}{2})$	2.088	$\nu(4d\frac{5}{2}\frac{3}{2}) \to \pi(4d\frac{3}{2}\frac{3}{2})$	4.380	
	$\nu(4g\frac{7}{2}\frac{3}{2}) \to \pi(4g\frac{7}{2}\frac{1}{2})$	3.362					
$^{160}\mathrm{Gd}$	$\nu(6i\frac{13}{2}\frac{5}{2}) \to \pi(6i\frac{11}{2}\frac{3}{2})$	2.222	$\nu(4d\frac{5}{2}\frac{3}{2}) \to \pi(4d\frac{5}{2}\frac{1}{2})$	2.551	$\nu(4d\frac{5}{2}\frac{3}{2}) \to \pi(4d\frac{3}{2}\frac{3}{2})$	1.028	
	$\nu(4g\frac{9}{2}\frac{7}{2}) \to \pi(4g\frac{9}{2}\frac{9}{2})$	1.622	$\nu(5h\frac{11}{2}\frac{1}{2}) \to \pi(5h\frac{9}{2}\frac{3}{2})$	1.362	$\nu(4d\frac{3}{2}\frac{1}{2}) \to \pi(4d\frac{3}{2}\frac{3}{2})$	1.204	
			$\nu(6i\frac{13}{2}\frac{1}{2}) \to \pi(6i\frac{11}{2}\frac{3}{2})$	9.922			

TABLE III: Here are listed the strengths carried by the pnQRPA states contributing to the first, second and third (if any) peaks from the upper panels of Figs.2-9. On the left side of these numbers the 2qp configurations closest in energy to the corresponding pnQRPA states, are given. Actually this is the dominant configuration of the chosen pn phonon state.

Nucleus	1st peak		2nd peak		3rd peak		
	Transition	Strength	Transition	Strength	Transition	Strength	
²³² Th	$\nu(5h\frac{9}{2}\frac{7}{2}) \to \pi(5h\frac{9}{2}\frac{9}{2})$	1.810	$\nu(4d\frac{3}{2}\frac{3}{2}) \to \pi(4d\frac{3}{2}\frac{1}{2})$	1.900	$\nu(5p\frac{3}{2}\frac{1}{2}) \to \pi(5p\frac{3}{2}\frac{3}{2})$	2.548	
	$\nu(5f\frac{5}{2}\frac{1}{2}) \to \pi(5f\frac{5}{2}\frac{3}{2})$	1.569	$\nu(5h\frac{9}{2}\frac{3}{2}) \to \pi(5h\frac{11}{2}\frac{5}{2})$	9.913			
			$\nu(5h\frac{11}{2}\frac{3}{2}) \to \pi(5h\frac{9}{2}\frac{5}{2})$	7.157			
			$\nu(5h\frac{11}{2}\frac{5}{2}) \to \pi(5h\frac{9}{2}\frac{3}{2})$	2.190			
			$\nu(6i\frac{13}{2}\frac{5}{2}) \to \pi(6i\frac{11}{2}\frac{7}{2})$	2.392			
			$\nu(5h\frac{11}{2}\frac{7}{2}) \to \pi(5f\frac{11}{2}\frac{5}{2})$	8.709			
$^{238}\mathrm{U}$	$\nu(6g\frac{9}{2}\frac{3}{2}) \to \pi(6g\frac{7}{2}\frac{1}{2})$	2.253	$\nu(6i\frac{13}{2}\frac{3}{2}) \to \pi(6i\frac{13}{2}\frac{1}{2})$	4.259	$\nu(5p\frac{3}{2}\frac{1}{2}) \to \pi(5p\frac{3}{2}\frac{1}{2})$	1.397	
	$\nu(6i\frac{13}{2}\frac{1}{2}) \to \pi(6i\frac{13}{2}\frac{1}{2})$	1.079	$\nu(6i\frac{13}{2}\frac{3}{2}) \to \pi(6i\frac{11}{2}\frac{5}{2})$	2.868			
	$\nu(5f\frac{5}{2}\frac{1}{2}) \to \pi(5f\frac{5}{2}\frac{3}{2})$	1.888	$\nu(5h\frac{9}{2}\frac{3}{2}) \to \pi(5h\frac{9}{2}\frac{1}{2})$	1.112			
			$\nu(5h\frac{9}{2}\frac{1}{2}) \to \pi(5h\frac{9}{2}\frac{3}{2})$	6.201			
			$\nu(5h\frac{9}{2}\frac{1}{2}) \to \pi(5h\frac{9}{2}\frac{1}{2})$	2.912			
			$\nu(4d\frac{5}{2}\frac{5}{2}) \to \pi(4d\frac{5}{2}\frac{3}{2})$	2.019			
			$\nu(6g\frac{9}{2}\frac{1}{2}) \to \pi(6g\frac{7}{2}\frac{3}{2})$	3.662			
			$\nu(5f\frac{7}{2}\frac{1}{2}) \to \pi(5f\frac{5}{2}\frac{3}{2})$	1.222			

TABLE IV: Continuation of Table III.

Nucleus	1st peak		2nd peal	k	3rd peak		
	pnQRPA energy	Strength	pnQRPA energy	Strength	pnQRPA energy	Strength	
$^{76}\mathrm{Ge}$	7.033	1.084	10.850	1.740	12.602	1.718	
			11.605	3.371			
$^{82}\mathrm{Se}$	6.939	1.554	10.920	4.501	11.701	1.686	
					12.291	3.310	
$^{148}\mathrm{Nd}$	9.397	1.077	12.028	1.453			
	10.047	1.141	12.269	12.437			
			12.429	1.015			
$^{150}\mathrm{Nd}$	8.600	1.901	11.263	1.246	12.939	5.386	
			11.531	1.178	13.217	2.370	
			12.281	1.087			
			12.597	7.647			
$^{154}\mathrm{Sm}$	10.475	1.220	11.986	4.214	13.189	1.537	
	11.047	1.031	12.696	2.088	13.303	4.380	
	11.434	3.362					
$^{160}\mathrm{Gd}$	10.748	2.222	12.457	2.551	15.334	1.028	
	11.163	1.622	12.857	1.362	15.850	1.204	
			13.369	9.927			

TABLE V: The energies of the pnQRPA states which give the largest strength contributions to the peaks in Figs. 2-9, upper panels. The carried strengths are also given.

Nucleus	1st peak		2nd peal	k	3rd peak		
	pnQRPA energy Strength p		pnQRPA energy	Strength	pnQRPA energy	Strength	
²³² Th	12.895	1.810	15.622	1.900	19.559	2.548	
	13.578	1.569	15.952	9.913			
			16.367	7.157			
			16.593	2.190			
			16.731	2.392			
			16.942	8.709			
$^{238}\mathrm{U}$	13.641	2.253	16.079	4.259	21.137	1.397	
	14.792	1.079	16.306	2.868			
	15.219	1.888	16.452	1.112			
			16.559	6.201			
			16.613	2.912			
			16.831	2.019			
			17.391	3.662			
			18.232	1.222			

TABLE VI: Continuation of Table V.

Nucleus	1st peak		2nd peak		3rd peak		
	Transition Strength		Transition	Strength	Transition	Strength	
$^{76}\mathrm{Se}$	$\pi(3f\frac{7}{2}\frac{7}{2}) \to \nu(3f\frac{5}{2}\frac{5}{2})$	0.313	$\pi(3f\frac{7}{2}\frac{5}{2}) \to \nu(3f\frac{5}{2}\frac{5}{2})$	0.116	$\pi(3f\frac{5}{2}\frac{5}{2}) \to \nu(3f\frac{7}{2}\frac{3}{2})$	0.013	
			$\pi(3f\frac{7}{2}\frac{5}{2}) \to \nu(3f\frac{5}{2}\frac{3}{2})$	0.027			
			$\pi(3f\frac{7}{2}\frac{3}{2}) \to \nu(3f\frac{5}{2}\frac{5}{2})$	0.021			
$^{82}\mathrm{Kr}$	$\pi(3f\frac{7}{2}\frac{7}{2}) \to \nu(3f\frac{5}{2}\frac{5}{2})$	0.135	$\pi(3p\frac{3}{2}\frac{3}{2}) \to \nu(3p\frac{1}{2}\frac{1}{2})$	0.118	$\pi(3f\frac{7}{2}\frac{3}{2}) \to \nu(3f\frac{5}{2}\frac{5}{2})$	0.019	
$^{148}\mathrm{Sm}$	$\pi(5h\frac{11}{2}\frac{3}{2}) \to \nu(5h\frac{9}{2}\frac{1}{2})$	0.139	$\pi(4d\frac{5}{2}\frac{1}{2}) \to \nu(4d\frac{3}{2}\frac{1}{2})$	0.037	$\pi(4g\frac{9}{2}\frac{7}{2}) \to \nu(4g\frac{7}{2}\frac{5}{2})$	0.011	
	$\pi(5h\frac{11}{2}\frac{3}{2}) \to \nu(5h\frac{9}{2}\frac{3}{2})$	0.151	$\pi(4g\frac{9}{2}\frac{9}{2}) \to \nu(4g\frac{7}{2}\frac{7}{2})$	0.017	$\pi(4g\frac{7}{2}\frac{3}{2}) \to \nu(4g\frac{9}{2}\frac{5}{2})$	0.012	
	$\pi(5h\frac{11}{2}\frac{3}{2}) \to \nu(5h\frac{9}{2}\frac{3}{2})$	0.165					
$^{150}\mathrm{Sm}$	$\pi(5h\frac{11}{2}\frac{3}{2}) \to \nu(5h\frac{9}{2}\frac{1}{2})$	0.227	$\pi(5h\frac{9}{2}\frac{1}{2}) \to \nu(5h\frac{9}{2}\frac{3}{2})$	0.012			
	$\pi(5h\frac{11}{2}\frac{1}{2}) \to \nu(5h\frac{9}{2}\frac{3}{2})$	0.134	$\pi(4d\frac{5}{2}\frac{1}{2}) \to \nu(4d\frac{3}{2}\frac{1}{2})$	0.018			
	$\pi(5h\frac{11}{2}\frac{3}{2}) \to \nu(5h\frac{9}{2}\frac{3}{2})$	0.103					
$^{154}\mathrm{Gd}$	$\pi(4d\frac{5}{2}\frac{3}{2}) \to \nu(4d\frac{3}{2}\frac{3}{2})$	0.081	$\pi(5h\frac{11}{2}\frac{3}{2}) \to \nu(5h\frac{9}{2}\frac{3}{2})$	0.061	$\pi(5h\frac{11}{2}\frac{3}{2}) \to \nu(5h\frac{9}{2}\frac{1}{2})$	0.039	
	$\pi(5h\frac{11}{2}\frac{5}{2}) \to \nu(5h\frac{9}{2}\frac{5}{2})$	0.140	$\pi(5h\frac{11}{2}\frac{1}{2}) \to \nu(5h\frac{9}{2}\frac{3}{2})$	0.046	$\pi(4d\frac{5}{2}\frac{1}{2}) \to \nu(4d\frac{3}{2}\frac{3}{2})$	0.019	
					$\pi(4g\frac{9}{2}\frac{7}{2}) \to \nu(4g\frac{7}{2}\frac{7}{2})$	0.016	
¹⁶⁰ Dy	$\pi(4d\frac{5}{2}\frac{3}{2}) \to \nu(4d\frac{3}{2}\frac{3}{2})$	0.050	$\pi(5h\frac{9}{2}\frac{1}{2}) \to \nu(5h\frac{9}{2}\frac{3}{2})$	0.067	$\pi(6i\frac{13}{2}\frac{1}{2}) \to \nu(6i\frac{11}{2}\frac{3}{2})$	0.063	
	$\pi(5h\frac{11}{2}\frac{5}{2}) \to \nu(5h\frac{9}{2}\frac{5}{2})$	0.076	$\pi(4g\frac{9}{2}\frac{9}{2}) \to \nu(5h\frac{7}{2}\frac{7}{2})$	0.113	$\pi(4d\frac{5}{2}\frac{1}{2}) \to \nu(4d\frac{3}{2}\frac{3}{2})$	0.051	
	$\pi(5h\frac{9}{2}\frac{3}{2}) \to \nu(6i\frac{9}{2}\frac{5}{2})$	0.365	$\pi(6i\frac{13}{2}\frac{3}{2}) \to \nu(6i\frac{11}{2}\frac{1}{2})$	0.059	$\pi(5h\frac{11}{2}\frac{3}{2}) \to \nu(5h\frac{9}{2}\frac{3}{2})$	0.054	
			$\pi(5h\frac{11}{2}\frac{5}{2}) \to \nu(5h\frac{9}{2}\frac{3}{2})$	0.073			
$^{232}\mathrm{U}$	$\pi(6i\frac{11}{2}\frac{7}{2}) \to \nu(6i\frac{13}{2}\frac{5}{2})$	0.011	$\pi(6i\frac{13}{2}\frac{5}{2}) \to \nu(6i\frac{11}{2}\frac{5}{2})$	0.031	$\pi(6i\frac{13}{2}\frac{5}{2}) \to \nu(6i\frac{11}{2}\frac{3}{2})$	0.008	
	$\pi(6i\frac{13}{2}\frac{5}{2}) \to \nu(6i\frac{11}{2}\frac{5}{2})$	0.013					
	$\pi(6i\frac{13}{2}\frac{5}{2}) \to \nu(6i\frac{11}{2}\frac{3}{2})$	0.011					
²³⁸ Pu	$\pi(6i\frac{11}{2}\frac{7}{2}) \to \nu(6i\frac{13}{2}\frac{7}{2})$	0.008	$\pi(6i\frac{13}{2}\frac{1}{2}) \to \nu(6i\frac{11}{2}\frac{1}{2})$	0.010	$\pi(6i\frac{11}{2}\frac{7}{2}) \to \nu(6i\frac{13}{2}\frac{5}{2})$	0.005	
	$\pi(5f\frac{5}{2}\frac{3}{2}) \to \nu(5f\frac{5}{2}\frac{5}{2})$	0.009					

TABLE VII: The same as in Table III but for the lower panels of Figs. 2-9.

Nucleus	s 1st peak pnQRPA energy Strength p		2nd peal	k	3rd peak	
			pnQRPA energy	Strength	pnQRPA energy	Strength
$^{76}\mathrm{Se}$	2.684	0.313	4.904	0.116	13.028	0.013
			6.169	0.027		
			6.627	0.021		
$^{82}{ m Kr}$	2.158	0.135	5.313	0.118	8.172	0.019
$^{148}\mathrm{Sm}$	2.196	0.139	6.209	0.037	10.029	0.011
	2.301	0.151	7.408	0.017	11.899	0.012
	2.427	0.165				
$^{150}\mathrm{Sm}$	3.051	0.227	6.420	0.012		
	3.102	0.134	7.369	0.018		
	3.419	0.103				
$^{154}\mathrm{Gd}$	2.071	0.081	3.169	0.061	3.928	0.039
	2.491	0.140	3.600	0.046	4.170	0.019
					4.401	0.016
$^{160}\mathrm{Dy}$	4.587	0.05	5.616	0.067	6.209	0.063
	4.756	0.076	5.742	0.113	7.469	0.051
	5.392	0.365	5.830	0.059	7.559	0.054
			5.968	0.072		
$^{232}{ m U}$	3.107	0.011	9.531	0.031	16.069	0.008
	4.917	0.013				
	6.656	0.011				
²³⁸ Pu	3.378	0.008	11.751	0.010	17.689	0.005
	3.415	0.009				

TABLE VIII: The same as in Table V, but for the lower panels of Figs. 2-9.

Of course, this feature is mainly caused by the fact that while for Ge and Se transitions the states contributing to the GT resonance have an energy separated by a gap from the upper two qp dipole configurations, in the heavier nuclei such energy gap does not exist due to both deformation effect on single particle energies and the fact that the last filled state is far away from a major shell closure.

In Tables III and IV we list the single particle β^- transitions characterized by the fact that the corresponding two quasiparticle energy is the closest one to a pnQRPA state contributing to the n-th peak with the strength given at its right side. The pnQRPA energies for the states bringing the strength listed in Tables III and IV are given in Tables V and VI, respectively.

The single particle transitions $\nu(nljI) \to \pi(nlj'I')$ which coherently contribute to the collective transition $0^+ \to 1^+$, are characterized by the change of quantum numbers j and I by at most one unit i.e. $|\Delta j|=0,1$ and $|\Delta I|=0,1$. The $(\Delta j,\Delta I)$ values for the single particle transition which represents the dominant component of the pnQRPA state which carries the maximal strength in a GT resonance are (1,1) (76 Ge), (0,1)(82 Se), (0,1) (148 Nd), (0,1)(150 Nd), (1,0) (154 Sm), (1,1) (160 Gd), (1,1) (232 Th), (0,1)(238 U). From Tables III and IV, it results that the GT resonances are admixtures of $\Delta I + \Delta j = 1, 2$ transitions.

A common feature for all nuclei considered in the present paper is that the dominant component of the pnQRPA state, i.e. that component which is excited with the largest probability by the GT transition operator, involves single particle states with small I. Indeed, such transitions $\nu I \to \pi I'$ have either I or I' equal to $\frac{1}{2}$ or $\frac{3}{2}$. In the cases of ¹⁵⁴Sm the angular momenta, involved in the transition are equal to each other. The common value is $\frac{3}{2}$. In Figs. 2-9 we give also the folded 2qp strength. One notes that the pnQRPA correlations push the strength to the higher energy. One of the main effects, comparing it with the 2qp picture, is that it concentrates most of the strength in the GT resonance which is the most collective pn excitation in the intermediate odd-odd nucleus.

Now, let us focus our attention on the β^+ strength distribution in the daughter nuclei. These strengths are much weaker in magnitude than those characterizing the β^- strength in the mother nuclei. Another difference between the two processes is that for the single beta minus process the maximum strength is concentrated at relatively high energy, around the Gamow-Teller resonance, while in the beta plus decay, most of the strength lies around 5 MeV. Indeed, from the lower panels of Figs. 2-9, one sees that the first peak, is the highest one. Exception from this rule is 232 Th where the β^+ strength is quite small and

its distribution has a peak lying around the energy of 10 MeV. Switching on the QRPA correlations one notices a decrease of the 2qp strength. Actually the difference in strengths which appear for the peaks is distributed among the remaining pnQRPA states, the total amount of strength in the two pictures being the same. The two qp configurations which contribute most to the first peaks shown in Figs. 2-9, are listed in Table VII. They are the dominant components of pnQRPA states with the energies given in Table VIII. As in the case of the single β^- decay of the mother nuclei, here also most of the dominant transitions take place between states of low angular momenta $(I = \frac{3}{2}, \frac{1}{2})$. However, due to the small magnitude of the transition strengths here one notices several transitions between states with angular momenta equal to $\frac{5}{2}$, $\frac{7}{2}$, $\frac{9}{2}$.

Inspecting the expression of the double beta transition amplitude, one notes that the numerator of a chosen term from the sum, has three factors: i) one which determines the strength of the β^- transition to a particular state $|1_k\rangle_i$, ii) one whose hermitian conjugate matrix element describes the β^+ transition to a state $|1_{k'}\rangle_f$ and iii) the overlap of the states reached by the decay of the initial and final nuclei, respectively. One expects that the maximum contribution to the GT transition amplitude M_{GT} is achieved when the two single beta matrix elements are maximal and moreover the overlaps of the dipole states in the odd-odd system is maximum. Therefore, we could ask ourselves whether among the peaks in the upper panels and those of the lower panels there are pairs of peaks determined by states of maximal overlap. From Tables III and VII one could identify many such pairs of peaks from the beta minus and beta plus strength distributions. For illustration we mention only one example. In ¹⁴⁸Nd the maximum contribution to the GT resonance is brought by the pnQRPA state of energy equal to 12.269MeV. Indeed, the corresponding strength is 12.437 and moreover this is the leading strength. The dominant amplitude for this state corresponds to the single particle transition $\nu(4g\frac{9}{2}\frac{5}{2}) \to \pi(4g\frac{7}{2}\frac{3}{2})$. On the other hand the strength distribution for 148 Sm shows a third peak determined by the pnQRPA state of energy equal to 11.899 MeV. Since the dominant two quasiparticle component of this collective state, corresponds to the single particle transition $\pi(4g\frac{7}{2}\frac{3}{2}) \rightarrow \nu(4g\frac{9}{2}\frac{5}{2})$, as shown in Table VII, one expects that the overlap of the pnQRPA states mentioned above is maximally large.

The single beta decays strengths of a given nucleus satisfy the N-Z sum rule, known under the name of Ikeda sum rule [38]. Our predictions for β^- and β^+ strengths satisfy the

Ikeda sum rule in the heavy isotopes while for 76 Ge and 82 Se small deviations of 3 and 1.7% respectively, are registered.

Let us analyze now the results for the double beta process, given in Table II. The dipole-dipole interaction strengths have been chosen as given by the empirical formula (4.4). The ratio of the pp and ph interaction strengths determines the g_{pp} factor. As we already mentioned before, this A dependence for the interaction strengths depends on single particle basis as well as on the truncation of the single particle space and therefore its validity for the present formalism is questionable. As a matter of fact for the lightest nuclei a larger value for χ approaches better the experimental situation while for ²³⁸U a smaller value is more suitable. Definitely, the safe way of fixing the ph and pp interaction strengths would be to fit the position of GT resonance centroid of the odd-odd intermediate nucleus and the half-lives of the β^+ decay of the of unstable nuclei in this mass region, respectively. However since for the cases considered here the experimental data mentioned above are lacking, we adopted the empirical formula (4.4) just to obtain some reference results to be compared with the ones obtained with the same interaction but different single particle basis.

The denominator from the equation defining M_{GT} involves the $Q_{\beta\beta}$ values and the experimental energy of the first 1⁺. These values are given in Table IX. Except for the case

Nucleus	$^{76}\mathrm{Ge}$	$^{82}\mathrm{Se}$	$^{148}\mathrm{Nd}$	$^{150}\mathrm{Nd}$	$^{154}\mathrm{Sm}$	$^{160}\mathrm{Gd}$	$^{232}\mathrm{Th}$	$^{238}{ m U}$
$Q_{\beta\beta}[{ m MeV}]$	2.04	3.01	1.93	3.37	1.25	1.73	0.85	1.15
Nucleus	$^{76}\mathrm{As}$	$^{82}\mathrm{Br}$	$^{148}\mathrm{Pm}$	$^{150}\mathrm{Pm}$	$^{154}\mathrm{Eu}$	$^{160}\mathrm{Tb}$	²³² Pa	$^{238}\mathrm{Np}$
$E_{1+}[keV]$	44	75	137	137*	72	139	1000*	244

TABLE IX: The $Q_{\beta\beta}$ -values for mother nuclei are given in units of MeV. In the lowest row, the experimental energy for the first 1^+ states in the intermediate nuclei are given in units of keV.*) For 150 Pm and 232 Pa there are not available data. Therefore we take the ad hoc values characterized by an asterisk. Actually changing E_{1^+} within 1 MeV does not modify the order of magnitude of $T_{1/2}$

of (⁷⁶Ge; ⁷⁶Se) all other pairs of (mother;daughter) nuclei are characterized by only slightly different nuclear deformations. For this reason in our calculations the nuclear deformations of mother and daughter nuclei have been considered equal to each other. The results for

 M_{GT} and $T_{1/2}$ are listed in Table II. They are compared with the experimental available data as well as with the predictions of those of Ref.[28]. Table II shows a good agreement between the predicted $T_{1/2}$ for ⁸²Se and ²³⁸U, and the corresponding experimental half life given in Ref.[31, 32, 33] and Ref.[21, 22, 33], respectively. Our prediction for the half life of ¹⁵⁰Nd is 69 times lower than the corresponding lower experimental limit. As shown in the second row for this nucleus, this discrepancy can be recovered by changing g_{pp} to a value equal to 1.50. In this context we would like to mention that while for the lightest two nuclei from Table II, the M_{GT} function of g_{pp} shows a very abrupt decreasing part, for the heavier nuclei the cancellation point is reached with a curve of a moderate slope. In the case of ¹⁵⁰Nd the cancellation value of g_{pp} is larger than 1.8 and therefore the adjusted value of 1.5 is still far away from the critical point where the pnQRPA breaks down.

The predicted half life of ⁷⁶Ge shown in the first row of Table II is only slightly smaller than the lower limit of the corresponding experimental data. For this case, however, the deformations for mother and daughter given in Ref. [40] are quite different from each other. This feature challenged us to consider in our calculations different deformations for ⁷⁶Ge and ⁷⁶Se. Therefore, we repeated the calculations for the decay of ⁷⁶Ge with the deformation $d_m = 1.6$ for the mother and $d_d = 1.9$ for the daughter nucleus. The pairing strengths for the new value for the nuclear deformation acquired by the mother nucleus are G_p =0.290, G_n =0.280. The results are shown in the second row of Table II. From there one remarks a good agreement with the experimental data for $T_{1/2}$.

To conclude, considering different deformations for mother and daughter nuclei decreases the overlap matrix elements involved in M_{GT} . Due to this effect the $T_{1/2}$ value is increased. It is an open question whether considering different deformations for 150 Nd and 150 Sm would wash out the big discrepancy with the experimental data shown in the first row for the decay of 150 Nd. At the first glance one may say that in order to have a positive answer to the question formulated above, one needs a larger difference between the two deformations than indicated in Refs. [39,40]. Since the half life is sensitive to the pairing properties one may suspect that for this case the proton-neutron pairing might play an important role.

Comparing the results for $T_{1/2}$ obtained with our formalism with those obtained in Ref.[28] by a different method one notices that for four emitters, ¹⁴⁸Nd, ¹⁵⁰Nd, ¹⁵⁴Sm, ¹⁶⁰Gd, our predicted half lives are shorter than in the above quoted reference while for the remaining nuclei the ordering of the half lives is opposite. In some cases the difference between the two

sets of predictions are in the range of two orders of magnitudes. Since the two methods are based on different approaches for the transition amplitudes, it is an open question whether these big discrepancies could get a consistent justification.

Finally we addressed the question of how the GT transition amplitude depends on g_{pp} and whether this dependence is influenced by the nuclear deformations. The results of our investigation are presented in Figs. 12, 13. The input parameters of single particle states and pairing interactions are those of ⁷⁶Ge. From Fig.12 one sees that for small values of $g_{pp} (\leq 0.5), M_{GT}$ depends monotonically on d while for $g_{pp} \geq 0.5$ this property is lost. The repulsive character of the pp interaction causes the cancellation of M_{GT} for a g_{pp} around 3. As seen from Fig. 12 the cancellation point depends on deformation. Also the curves look of Fig 12 is not changed, the value of g_{pp} where M_{GT} is canceled is quenched by the factor by which the strength χ is increased when one passes from Fig.12 to Fig.13. In this context we recall that for spherical nuclei, the cancellation, corresponding to the value of χ which reproduces the position of the GT resonance, takes place for $g_{pp} \approx 1$. For this value the relation between the matrix elements of the ph and pp two body interactions is given by the Pandya transformation. From Fig. 13 it results that the cancellation points depend, as we already said, on deformation. It is an open question whether the deformation dependence of the GT resonance is such that the cancellation point of M_{GT} is always brought to about 1.

V. SUMMARY AND CONCLUSIONS

The main results described in the previous sections can be summarized as follows. The two neutrino double beta decay transition amplitudes and half lives for eight isotopes have been calculated within a pnQRPA approach based on a projected spherical single particle basis.

The single particle energies are approximated by averaging a particle-core Hamiltonian on the projected basis. Due to the fact that the core volume conservation is properly taken into account, the resulting energies depend on deformation in a similar manner as Nilsson levels. This feature suggests that the results for two neutrino double beta decay rate provided by a pnQRPA formalism with such a basis will be essentially different than those obtained in Ref.[9] where single particle energies depend linearly on deformation.

First we studied the β^- and β^+ strength distributions for mother and daughter nuclei respectively. Both types of strengths are fragmented due to the nuclear deformation. The position as well as the width of the GT resonance depend on nuclear mass. Moreover, while the GT resonance lies in the upper part of the pnQRPA energy spectrum (the meaning of this statement is that beyond the GT resonance there is only a little strength left to be distributed) the highest peak in the folded strength distribution plot for the β^+ decay appears always for low energies. This feature suggests that the GT resonance is mainly influenced by the ph while the peak in the β^+ strength distribution, by the pp channels of the dipole-dipole two-body interaction. It seems that there is a correspondence between the pnQRPA states of mother and daughter nuclei contributing most to the folded strength distributions. The associated states, due to the correspondence mentioned above, have maximal overlap and therefore give the main contribution to the M_{GT} value. From Figs. 2-9 one remarks that the GT resonance strength depend on the atomic mass. The larger A, the larger the height of the resonance. Moreover the energy of the resonance center is also an increasing function of A. For two emitters, ⁸²Se and ¹⁵⁴Sm, the GT resonance has a doublet structure. This reminds us of the doublet structure of the dipole giant charge preserving resonances due to the coupling to the quadrupole degrees of freedom. Actually in this case also the doublet structure is a deformation effect and by this an effect caused by the quadrupole coordinates of the core.

The M_{GT} and $T_{1/2}$ values have been first calculated by considering equal deformations for mother and daughter nuclei. The A dependence of the ph and pp proton-neutron dipole interaction is taken as in Ref.[11]. The agreement with experimental data concerning the $T_{1/2}$ value of 82 Se and 238 U is very good good. The result for 76 Ge is slightly smaller than the experimental data. The discrepancy was removed by considering the deformation for 76 Ge different from that of 76 Se. Indeed, this is the only case where according to Refs.[30,40] the deformations for the two nuclei involved in the double beta decay are quite different. To bring the theoretical value of $T_{1/2}$ for 150 Nd in agreement with the experimental data one needs a larger deformation difference than given in literature [39,40]. Moreover, the pairing strength should deviate very much from what the difference of neighboring even-even isotopes masses requires. Due to this feature for this case we reproduced the experimental half life by changing g_{pp} from 0.11154 to 1.5. Note that the critical value of g_{pp} for this isotope is 1.8. It is noteworthy that for isotopes, 76 Ge, 82 Se, 238 U, where the calculated

half lives agree with the corresponding experimental data the values used for g_{pp} are small which results in having a small effect coming from the pp interaction on this observable. As shown in Table II for 238 U, cancelling g_{pp} does not alter the agreement with the experimental data. Then it arises the question whether the pp interaction is really needed at all in order to describe quantitatively the double beta decay process. Is the large sensitivity of the single β^+ matrix elements, pointed out for the first time by Cha in Ref.[41], a real effect or just an artifact caused by the instability of the pnQRPA ground state [8]? As shown in Table II for 76 Ge, taking different deformations for mother and daughter nuclei brings an important effect on $T_{1/2}$ but not a dramatic change as claimed in Ref. [42]. The difference between the two descriptions consists in the fact that here the overlap matrix elements of the states in the mother and daughter nuclei are estimated in a manner consistent with the pnQRPA approach, while in the quoted reference the phonon operators are dissociated and the overlaps are calculated within the BCS and particle representations. Of course, in the latter case it is not possible to get a real hierarchy of the effects involved.

As we stressed in Ref.[19], going beyond pnQRPA approach, some forbidden processes might become possible. As an example, we studied the double beta transition on excited collective states. In the near future we shall investigate whether increasing the deformation for the daughter nuclei would substantially increase the reduced decay probability for such processes.

VI. APPENDIX A

In order to calculate the overlap matrix which enter the M_{GT} expression, we have to express the phonon operator for the mother nucleus in terms of the phonon operator of the daughter nucleus, following the boson expansion procedure [19].

$$\Gamma_{1\mu}^{\dagger}(i,k) = \sum_{k'} [W_i^f(k,k')\Gamma_{1\mu}^{\dagger}(f,k') + Z_i^f(k,k')\Gamma_{1,-\mu}(f,k')(-)^{1-\mu}]. \tag{A.1}$$

where the amplitudes W and Z can be easily calculated as follows:

$$W_{i}^{f}(k, k') = {}_{i}\langle 0|[\Gamma_{1\mu}(f, k'), \Gamma_{1\mu}^{\dagger}(i, k)]|0\rangle_{f},$$

$$Z_{i}^{f}(k, k') = {}_{i}\langle 0|[\Gamma_{1\mu}^{\dagger}(f, k), \Gamma_{1,-\mu}^{\dagger}(i, k')(-)^{1-\mu}]|0\rangle_{f}.$$
(A.2)

It is clear that once these amplitudes are calculated, the overlap matrix elements are readily obtained:

$$_{i}\langle 1_{k}|1_{k}^{\prime}\rangle_{f} = W_{i}^{f}(k,k^{\prime})_{i}\langle 0|0\rangle_{f} \tag{A.3}$$

provided that the overlap of the two vacua is known. In what follows we shall describe the necessary steps to derive the expressions of the two factors from the right hand side of the above expression. By a direct calculation one finds:

$$W_{i}^{f}(k,k')^{*} = (X_{k}(i;pn)X_{k'}(f;p'n') - Y_{k}(i;pn)Y_{k'}(f;p'n'))_{i}\langle 0|[A_{1\mu}(i;pn),A_{1\mu'}^{\dagger}(f;p'n')]|0\rangle_{f}$$

$$+ (X_{k}(i;pn)Y_{k'}(f;p'n') - Y_{k}(i;pn)X_{k'}(f;p'n'))_{i}\langle 0|[(-)^{1-\mu}A_{1-\mu}^{\dagger}(i;pn),A_{1\mu'}^{\dagger}(f;p'n')]|0\rangle_{f}$$
(A.4)

The symbol "*" stands for the complex conjugation operation. The matrix elements of the commutators of the two quasiparticle operators are expressed further in terms of the anti-commutator of the single particle operators which is calculated as explained in Ref.[14]:

$$\{c_{\alpha IM}(i), c_{\alpha'I'M'}^{\dagger}(f)\} = \mathcal{N}_{nlj}^{I}(i)\mathcal{N}_{n'l'j'}^{I'}(f) \sum_{J} (C_{I0I}^{1JI})^{2} (N_{J}^{(g)}(d))^{-1} (N_{J}^{(g)}(d'))^{-1} \times O_{J}^{(c)}(i, f)\delta_{II'}\delta_{jj'}\delta_{MM'} \equiv O_{if}^{\alpha I}\delta_{II'}\delta_{jj'}\delta_{\alpha\alpha'}\delta_{MM'}$$
(A.5)

Here $N_J^{(g)}$ denotes the norm of the core projected state:

$$\varphi_{JM}^{(g)}(d) = N_J^{(g)}(d) P_{M0}^J e^{d(b_{20}^{\dagger} - b_{20})} |0\rangle_b;; \tag{A.6}$$

where $|0\rangle_b$ denotes the vacuum state for the quadrupole bosons. The overlap matrix for the initial (i) and final (f) core states is denoted by $O_J^{(c)}(i, f)$, and has the expression:

$$O_J^{(c)}(i,f) \equiv \langle \varphi_{JM}(d) | \varphi_{JM}(d') \rangle = N_J^{(g)}(d) N_J^{(g)}(d') e^{-\frac{d^2 + d'^2}{2}} (2L + 1) I_J^{(0)}(\sqrt{dd'}). \tag{A.7}$$

where the factor $I_J^{(0)}$ is defined by Eq.(2.11). The initial nucleus deformation is denoted by d while d' stands for the deformation parameter characterizing the final nucleus. Note that in the limit $d' \to d$ we have

$$O_J^{(c)}(i,f) \rightarrow 1, , O_{if}^{\alpha I} \rightarrow 1.$$
 (A.8)

With these details, one further obtains:

$${}_{i}\langle 0|[A_{1\mu}(i;pn),A_{1\mu'}^{\dagger}(f;p'n')]|0\rangle_{f} = \delta_{I_{p}I_{p'}}\delta_{I_{n}I_{n'}}\delta_{\mu\mu'}(U_{p}^{m}U_{p}^{d}+V_{p}^{m}V_{p}^{d})(U_{n}^{m}U_{n}^{d}+V_{n}^{m}V_{n}^{d})O_{if}^{\alpha_{p}I_{p}}O_{if}^{\alpha_{n}I_{n}},$$
(A.9)

 ${}_{i}\langle 0|[(-)^{1-\mu}A_{1,-\mu}^{\dagger}(i;pn),A_{1\mu'}^{\dagger}(f;p'n')]|0\rangle_{f}=\delta_{I_{p}I_{p'}}\delta_{I_{n}I_{n'}}\delta_{\mu\mu'}(U_{p}^{m}V_{p}^{d}-V_{p}^{m}U_{p}^{d})(U_{n}^{m}V_{n}^{d}-V_{n}^{m}U_{n}^{d})O_{if}^{\alpha_{p}I_{p}}O_{if}^{\alpha_{n}I_{n}},$

Thus, the final expressions for the amplitudes W and Z are:

$$W_{i}^{f}(k,k') = \sum_{pn} \left[(X_{k}(i;pn)X_{k'}(f;pn) - Y_{k}(i;pn)Y_{k'}(f;pn))(U_{p}^{i}U_{p}^{f} + V_{p}^{i}V_{p}^{f})(U_{n}^{i}U_{n}^{f} + V_{n}^{i}V_{n}^{f}) \right.$$

$$+ \left. (X_{k}(i;pn)Y_{k'}(f;pn) - Y_{k}(i;pn)X_{k'}(f;pn))(U_{p}^{i}V_{p}^{f} - V_{p}^{i}U_{p}^{f})(U_{n}^{i}V_{n}^{f} - V_{n}^{i}U_{n}^{f}) \right] O_{if}^{\alpha_{p}I_{p}} O_{if}^{\alpha_{n}I_{n}}$$

$$Z_{i}^{f}(k,k') = \sum_{pn} \left[(X_{k}(i;pn)X_{k'}(f;pn) - Y_{k}(i;pn)Y_{k'}(f;pn))(U_{p}^{i}V_{p}^{f} - V_{p}^{i}U_{p}^{f})(U_{n}^{i}V_{n}^{f} - V_{n}^{i}U_{n}^{f}) \right. (A.11)$$

$$+ \left. (X_{k}(i;pn)Y_{k'}(f;pn) - Y_{k}(i;pn)X_{k'}(f;pn))(U_{p}^{i}U_{p}^{f} + V_{p}^{i}V_{p}^{f})(U_{n}^{i}U_{n}^{f} + V_{n}^{i}V_{n}^{f}) \right] O_{if}^{\alpha_{p}I_{p}} O_{if}^{\alpha_{n}I_{n}}.$$

As for the ground states overlap, the result is

and

$${}_{i}\langle 0|0\rangle_{f} \approx {}_{i}\langle BCS|BCS\rangle_{f}$$

$$= \prod_{n} \left[U_{p}^{i}U_{p}^{f} + V_{p}^{i}V_{p}^{f} \left(O_{if}^{\alpha_{p}I_{p}}\right)^{2} \right] \prod_{n} \left[U_{n}^{i}U_{n}^{f} + V_{n}^{i}V_{n}^{f} \left(O_{if}^{\alpha_{n}I_{n}}\right)^{2} \right]. \tag{A.12}$$

If the mother and daughter nuclei are characterized by the same nuclear deformation, the corresponding overlap matrix elements are obtained from the above formulae by replacing d' by d. A good approximation of the resulting equation is given by the expression:

$$_{i}\langle 1_{k}|1_{k'}\rangle_{f} = \sum_{pn} \left[X_{k}(i,pn)X_{k'}(f,pn) - Y_{k}(i,pn)Y_{k}(f,pn)\right].$$
 (A.13)

The drawback of the procedure described above is that both factors of Eq.A.3 are evaluated within the framework of the BCS approximation while the matrix elements describing the single β^{\pm} transitions are calculated within the pnQRPA approach. Moreover, due to the overlap factors $O_{if}^{\alpha I}$, even the border of BCS frame is crossed toward the particle representation. This inconsistency of the levels of approximations makes the method doubtful, since it is not possible to define an hierarchy of various effects[42]. For example one could take care of a negligible contribution otherwise ignoring an important one. However, extending

the spirit of the RPA approach to the case of different deformations for the initial and final nuclei one obtains:

$$W_{i}^{f}(k,k') = \sum_{pn} \left[X_{k}(i;pn) X_{k'}(f;pn) - Y_{k}(i;pn) Y_{k'}(f;pn) \right],$$

$${}_{i}\langle 0|0\rangle_{f} = 1 \tag{A.14}$$

In this way the overlap matrix and the matrix elements characterizing the initial and final nuclei are treated in an unitary fashion. The numerical calculations presented in the present paper correspond to the overlap matrix determined by Eq.(A.14). We postpone for a forth-coming paper, the description of the β^{\pm} matrix elements within a higher pnQRPA approach consistent with the procedure presented in this Appendix for calculating the overlap matrix elements.

- [1] J. Suhonen and O. Civitarese, Phys.Rep. **300** (1998) 123.
- [2] J.D. Vergados, Phys. Rep. **361** (2001) 1.
- [3] H. Primakof and S. Rosen, Rep. Prog. Phys. 22 (1959) 125.
- [4] W. C. Haxton and G. J. Stephenson, Jr. Prog. Part. Nucl. Phys. 12(1984) 409.
- [5] T. Tomoda, Re. Prog. Phys. **54** (1991) 53.
- [6] A. Faessler, Prog. Part. Nucl. Phys. **21** (1988) 183.
- [7] .H. V. Klapdor-Kleingrothaus, Sixty Years of Double Beta Decay, World Scientific, Singapore (2001).
- [8] A. A. Raduta, Prog. Part. Nucl. Phys. 48(2002) 233.
- [9] A. A. Raduta, A. Faessler and D.S. Delion, Nucl. Phys. A 564 (1993) 185; Phys. Lett.B 312 (1993) 13.
- [10] A. A. Raduta, D. S. Delion and A. Faessler, Nucl. Phys. A 617 (1997) 176.
- [11] H. Homma, E. Bender, M. Hirsch, K. Muto, H.V. Klapdor-Kleingrothaus and T. Oda, Phys. Rev. C54 (1996) 2972.
- [12] P.Sarriguren, E. Moya de Guerra, A. Escuderos, A. C. Carrizo, Nucl. Phys. A 635 (1998)55; P. Sarriguren, E. Moya de Guerra and A. Escuderos, Nucl. Phys. A658 (1999)13; Nucl.

- Phys. A 691 (2001) 631; Phys. Rev. C 64(2001) 064306; P. Sarriguren, E. Moya de Guerra,
 L. Pacearescu, A. Faessler, F. Simkovic and A. A. Raduta, Phys. Rev. C 67 (2003) 044313.
- [13] J. Engel, M. Bender, J. Dobaczewski, W. Nazariewicz and R. Surnam, Phys. Rev. C 60 (1999) 014302; M. Bender, J. Dobaczewski, J. Engel and W. Nazarewicz, Phys. Rev. C 65 (2002) 054322.
- [14] A. A. Raduta, D. S. Delion and N. Lo Iudice, Nucl. Phys. A 564 (1993) 185.
- [15] A. A. Raduta, N. Lo Iudice and I. I. Ursu, Nucl. Phys. **A584** (1995) 84.
- [16] A. A. Raduta, Al. H. Raduta and Ad. R. Raduta, Phys. Rev. B 59 (1999) 8209; A. A. Raduta,
 E. Garrido and E. Moya de Guerra, Eur. Phys. Jour. D 15 (2001) 65
- [17] A. A. Raduta, A. Escuderos and E. Moya de Guerra, Phys. Rev. C 65, 2002) 024312.
- [18] S.G.Nilsson, Mat. Fys. Medd. K. Dan. Vid. Selsk. 29 no. 16 (1955).
- [19] A.A.Raduta, A.Faessler and S.Stoica, Nucl. Phys. **A534** (1991) 149.
- [20] M. E. Rose, Elementary Theory of Angular Momentum (Wiley, New York, 1957).
- [21] V.I. Tretyak and Yu. G. Zdesenko, At. Data Nucl. Data Tabl. 80 (2002) 83
- [22] A.S.Barabash, Czech. J. Phys. **52** (2002) 567.
- [23] S.R. Elliot and P. Vogel, Ann. Rev. Nucl. Part. Sci. **52** (2002) 115.
- [24] P.Ring and P.Shuck, The Nuclear Many-Body Problem, Springer, 1980, p. 76.
- [25] N. Lo Iudice, A. A. Raduta and D.S. Delion, Phys. Rev. C 50 (1994) 127.
- [26] A.A.Raduta, I.I. Ursu and D.S.Delion, Nucl. Phys. A 475 (1987) 439.
- [27] H.V.Klapdor, Prog. Part. Nucl. Phys. 17 (1986) 419.
- [28] X.R. Wu, M. Hirsch, A. Staudt, H.V. Klapdor-Kleingrothaus, Cheng-Rui Ching and Tso-Hsui Ho, Commun. Theor. Phys. 20 (1993) 453.
- [29] H. S. Miley, F. T. Avignone, III, R.L. Brodzinski, J. I. Collar and J. H. Reeves, Phys. Rev. Lett. 65 (1990) 3092.
- [30] F. T. Avignone III et al., Phys. Lett. **256** (1991) 559.
- [31] T. Kirsten, E. Heusser, D. Kaether, J. Oehm, E. Pernicka, H. Richter, Preceedings of the International Symposium on Nuclear Beta Decays and Neutrino, T.Kotani, H. Ejiri, E. Takasugi(eds.),p.81. Singapore:World Scientific 1986.
- [32] O. K. Manuel, Preceedings of the International Symposium on Nuclear Beta Decays and Neutrino, T.Kotani, H. Ejiri, E. Takasugi(eds.),p.81. Singapore:World Scientific 1986.
- [33] S.R. Elliot, A. A. Hahn, M.K. Moe, Phys. Rev. Lett. **59** (1987) 2020.

- [34] R. Madey, B.S.Flanders, B.D. Anderson, A. R. Baldwin, J.W. Watson, S.M. Austin, C.C.Foster, H.V. Klapdor and K. Grotz, Phys. Rev. C40 (1989) 540.
- [35] R.L. Helmer et al., Phys. Rev. C 55 (1997) 2802.
- [36] A. A. Klimenko et al., Nucl. Instrum. and Meth. B16 (1986) 446.
- [37] A. L. Turkevich, T. E. Economou and G. A. Cowan, Phys. Rev. Lett. 67 (1991) 3211.
- [38] K.Ikeda, Prog. Theor. Phys. 31 (1964) 434; K.Ikeda, S. Fujita and J.I.Fujita, Phys. Lett. 3 (1963) 271; J. I. Fujita and K. Ikeda, Prog. Theor. Phys. 36 (1966) 288.
- [39] G. Audi and A.H. Wapstra, Nucl. Phys. A595 (1995) 409; G. Audi, O. Bersillon, J. Blachot and A. H. Wapstra, Nucl. Phys. A 624 (1997) 1.
- [40] G. A. Lalazissis, S. Raman and P. Ring, At. Data and Nucl. Data Tables 60 (1995) 177.
- [41] D. Cha, Phys. Rev. C27 (1987) 2269.
- [42] F. Simkovic, L. Pacearescu and A. Faessler, Nucl. Phys. A 733 (2004) 321.
- [43] *)Throughout this paper the Rose [20] convention for the Wigner Eckart theorem is used.



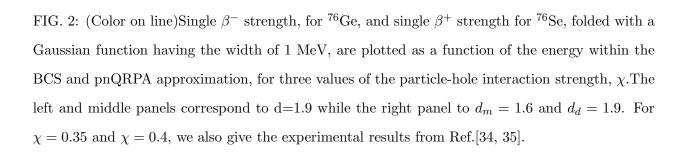




FIG. 4: The same as in Fig. 2, but for the β^- of $^{148}\mathrm{Nd}$ and the β^+ of $^{148}\mathrm{Sm}$.

FIG. 5: The same as in Fig. 2, but for the β^- of $^{150}\mathrm{Nd}$ and the β^+ of $^{150}\mathrm{Sm}$.

FIG. 6: The same as in Fig. 2, but for the β^- of $^{154}\mathrm{Sm}$ and the β^+ of $^{154}\mathrm{Gd}$.

FIG. 7: The same as in Fig. 2, but for the β^- of $^{160}\mathrm{Gd}$ and the β^+ of $^{160}\mathrm{Dy}$.

FIG. 8: The same as in Fig. 2, but for the β^- of 232 Th and the β^+ of 232 U.

FIG. 9: The same as in Fig. 2, but for the β^- of $^{238}\mathrm{U}$ and the β^+ of $^{238}\mathrm{Pu}$.

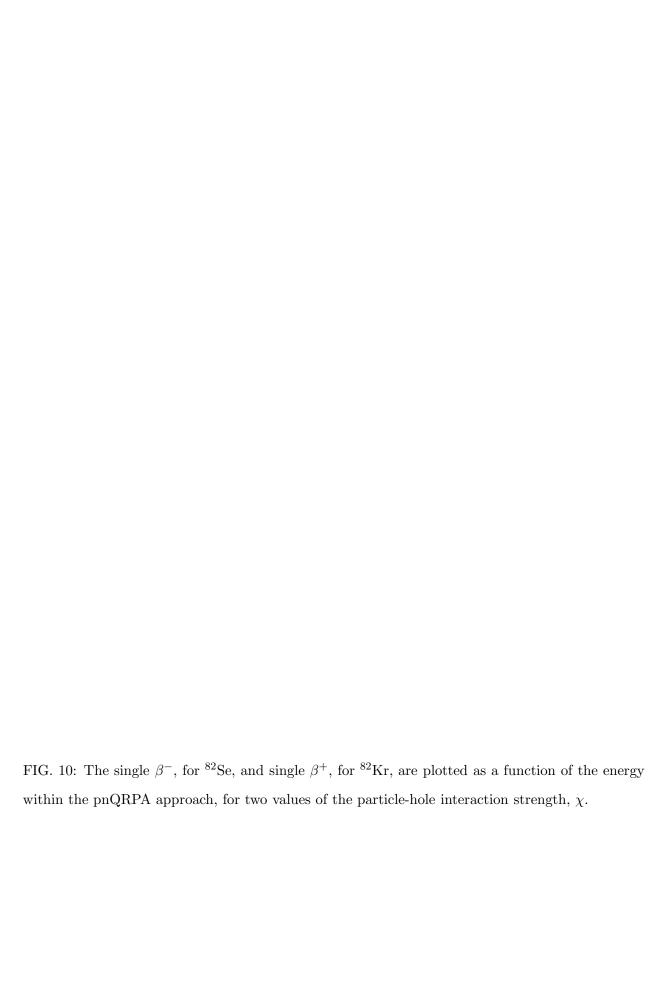


FIG. 11: The single β^- , for ²³²Th, and single β^+ , for ²³²U, are plotted as function of the energy within the pnQRPA approach, for $\chi=0.11$.

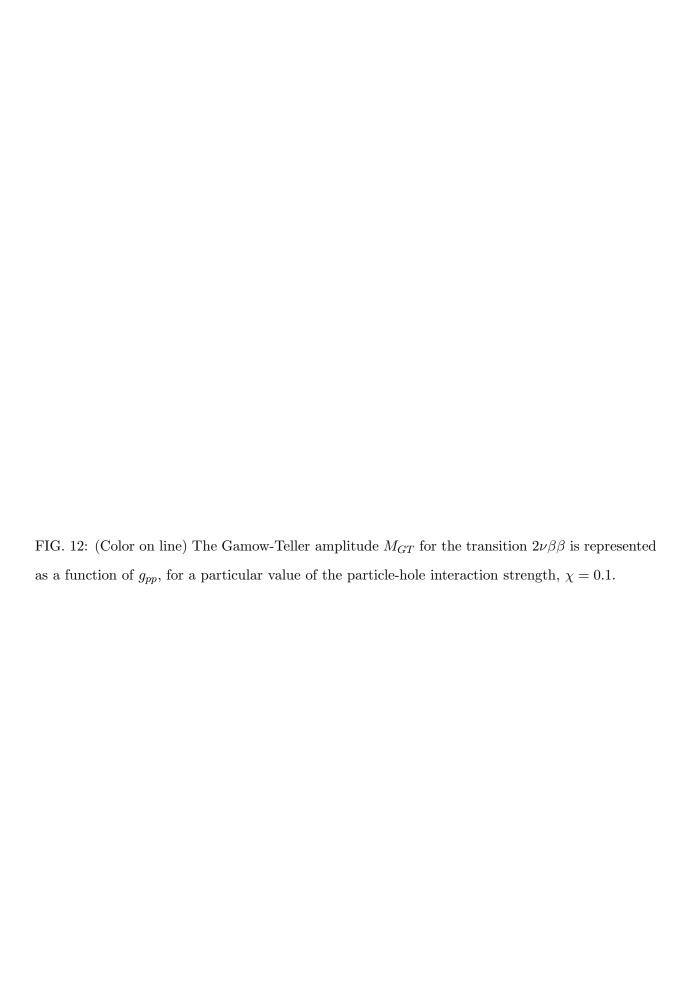


FIG. 13: (Color on line) The same as in Fig. 12 but for $\chi=0.3.$